UV-Spectrum Remote UVA Imaging for Use in Precision Agriculture

by

Megan HEATH

MANUSCRIPT-BASED THESIS PRESENTED TO ÉCOLE DE TECHNOLOGIE SUPÉRIEURE
IN PARTIAL FULFILLMENT OF A MASTER'S DEGREE
WITH THESIS IN ENVIRONMENTAL ENGINEERING
M.A.Sc.

MONTREAL, AUGUST 27TH, 2023

ÉCOLE DE TECHNOLOGIE SUPÉRIEURE
UNIVERSITÉ DU QUÉBEC

BOARD OF EXAMINERS

THIS THESIS HAS BEEN EVALUATED

BY THE FOLLOWING BOARD OF EXAMINERS

Mr. David St- Onge, Thesis supervisor
Department of Mechanical Engineering, École de Technologie Supérieure

Mr. Robert Hausler, Thesis Co-Supervisor
Department of Construction Engineering, École de Technologie Supérieure

Mrs. Ornwipa Thamsuwan, Chair, Board of Examiners
Department of Mechanical Engineering, École de Technologie Supérieure

Mrs. Josiane Nikieme, Member of the Jury
Department of Construction Engineering, École de Technologie Supérieure

Mr. Marco Pedersoli, Member of the Jury
Department of Systems engineering, École de Technologie Supérieure

THIS THESIS WAS PRESENTED AND DEFENDED

IN THE PRESENCE OF A BOARD OF EXAMINERS AND THE PUBLIC

ON JULY 25, 2023

AT ÉCOLE DE TECHNOLOGIE SUPÉRIEURE

ACKNOWLEDGEMENTS

Words cannot express my gratitude to my professors for their invaluable patience and feedback. I could only have undertaken this journey with my defence committee, who generously provided knowledge and expertise. Additionally, this endeavour would not have been possible without the generous support from the UTILI CREATE program, which financed my research.

I am also grateful to my colleagues for their editing help, late-night feedback sessions, and moral support. Thanks should also go to my research assistant, Ryan, and the people at Spiri Robotics, who generously hosted my internship, as they greatly impacted and inspired me.

Lastly, I should mention my family, especially my parents and partner. Their belief in me has kept my spirits and motivation high during this process. I also want to thank my dogs for the office company during Covid and their emotional support.

Interprétation algorithmique des polymorphismes spectraux UV floraux

Megan HEATH

RÉSUMÉ

La réflectance UV florale a longtemps été considérée comme un facteur essentiel dans les interactions plantes-pollinisateurs. Les pigments réfléchissant les UV sur les structures reproductives permettent aux pollinisateurs de localiser les fleurs depuis les airs et de différencier les espèces. Cette relation est possible grâce à la capacité des pollinisateurs, tels que les abeilles, à voir dans le spectre UV (300-400 nm). Malgré cette stratégie de signalisation visuelle bien documentée des plantes à fleurs, notre revue littéraire a indiqué que la réflectance spectrale UV est peu documentée pour plusieurs espèces cultivées. Sans tenir compte de cette particularité de la réflectance UV, les efforts de sélection pourraient rendre les fleurs difficiles à détecter pour les pollinisateurs artificiels, diminuant le rendement et la qualité de la récolte. Nous avons fait l'analyse spectrale des cultivars de fraisiers et comparés ces derniers à leur homologue sauvage. Les cultivars à fleurs blanches ont montré une plus grande visibilité des pollinisateurs, tandis que le cultivar à fleurs rouges était cryptique. La vision des abeilles (300-650nm) est adaptée pour détecter les fleurs. Ce projet s'inspire du spectre de vision des abeilles pour concevoir un détecteur inspiré de la nature (DIN) pour détecter à distance les fleurs de fraise. Deux algorithmes d'intelligence artificielle de pointe ont été entrainés sur un ensemble d'images de fleurs de fraises résultant en des performances supérieures de YOLOv5 par rapport à Faster R-CNN (mAP 0,978 contre 0,912, respectivement). Le DIN a ensuite été déployé sur un aéronef au-dessus d'un champ de fraises. Les résultats étaient comparables à l'état de l'art, mais notre DIN obtient un temps d'entraînement plus rapide (0,3 contre 5,5 heures) et une mAP plus élevée (0,951 contre 0,772). **Mots-clés:** detection remote, fleurs, fraises

UV-Spectrum Remote UVA Imaging for Use in Precision Agriculture

Megan HEATH

ABSTRACT

Floral UV-reflectance is considered an essential factor in plant-pollinator interactions. UV-reflective pigments on reproductive structures allow pollinators to locate flowers from the air and differentiate conspecifics. This relationship is possible due to the ability of pollinators, such as bees, to see in the UV spectrum (300-400nm). Despite this well-documented visual signalling strategy of flowering plants, our literary review indicated that few crop species have had their UV spectral reflectance documented. Without considering UV reflectance, breeding efforts could render flowers cryptic to pollinators, decreasing yield and harvest quality. Strawberry cultivars were spectrally analyzed and compared to their wild counterpart. White-flowering cultivars showed higher pollinator visibility, whereas the red-flowering cultivar was cryptic. Bee vision (300-650nm) is adapted to detect flowers. This project mimicked the bee vision range in designing and creating the Nature Inspired Detector (NID) to detect strawberry flowers remotely. Two state-of-the-art AI algorithms were trained on a custom strawberry flower image dataset where YOLOv5 outperformed Faster R-CNN(mAP 0.978 vs. 0.912, respectfully). The NID was then field deployed on a UAV over a strawberry field. Results were comparable to a contemporary study, but the NID had a faster training time (0.3 vs. 5.5 hrs) and higher mAP (0.951 vs. 0.772). **Keywords:** Remote detection, Flowers, Strawberry

TABLE OF CONTENTS

LIST OF TABLES

Page

LIST OF FIGURES

Page

LIST OF ABBREVIATIONS

CCD	Charge-coupled device
CFA	color filter array
CMOS	Complementary metal–oxide–semiconductor
CNN	Convolutional Neural Network
Faster R-CNN	Faster Region-based convolutional neural network
FN	False negative
FP	False positive
FReD	Floral Reflectance Database
GLCM	Grey level co-occurrence matrix
JPG	Joint Photographic Experts Group
LUX	the SI unit of illuminance, equal to one lumen per square meter
mAP	Mean average precision
RGB	Red, Green, Blue mosaic on photosensors
RPAS	Remotely Piloted Aircraft System
TP	True positive
UAV	Unmanned aerial vehicle
VGG16	Visual Geometry Group (16 layers)
YOLOv5	You only look once version 5.0

LIST OF ABBREVIATIONS

Angiosperm	A plant that has flowers and produces fruit
Seed	Fertilized plant offspring enclosed within a carpel
Bayer filter	A Bayer filter mosaic is a color filter array (CFA) for arranging RGB color filters on a square grid of photosensors.
Classification	A topic of pattern recognition in computer vision, is an approach of classification based on contextual information in images.
Contrast	Contrast is the difference in luminance or color that makes an object distinguishable
Convolutional filter	Convolution filters produce output images in which the brightness value at a given pixel is a function of some weighted average of the brightness of the surrounding pixels.
Cultivar	A plant variety that has been produced in cultivation by selective breeding
Drone	An aircraft without any human pilot, crew, or passengers on board
False Negative	A test result which incorrectly indicates that a particular condition or attribute is absent
False Positive	A test result which incorrectly indicates that a particular condition or attribute is present
Kernel	A filter that is used to extract the features from the images
Monochrome	Picture consisting of one channel (black and white)
Pixel value	Describes how bright and what color that pixel is
Precision (mAP)	Average precision computes the average precision value for recall value over 0 to 1

Precision Agriculture A farming management concept based on observing, measuring, and responding to inter and intra-field variability in crops

Random Forest An ensemble learning method for classification, regression and other tasks that operates by constructing a multitude of decision trees

Remote sensing The acquisition of information about an object or phenomenon without making physical contact with the object

Segmentation The process of partitioning a digital image into multiple image segments, also known as image regions

Spectral reflectance The reflectance measured at a given Ts and γ, within a small wavelength interval, $\delta\gamma$, centered at γ

Spectrophotometer An apparatus for measuring the intensity of light in a part of the light spectrum

[3cm]

LIST OF SYMBOLS AND UNITS OF MEASUREMENTS

λ	camera sensor pixel size
H	flight altitude in meters
c	Focal length
$\triangle$S	Contrast

INTRODUCTION

In recent decades, the rural exodus has drastically depleted the agricultural labour force and threatened the future of global food production. Traditionally, farmers rely on visual recognition of crop health, plant species, and soil needs. These are skills that are passed down generationally. The field of precision agriculture (PA) incorporates modern technology and cultivated knowledge to manage areas with minimal inputs, personal expertise and workforce.

In traditional agriculture, fields are treated uniformly, leading to the overuse of water and agrochemicals. The development and open access of ground positioning systems (GPS) and geographic information systems (GIS) led to booming advancement in zone-specific field management. Zhang et al. (2002) found in a worldwide review that PA reduced groundwater contamination from fertilizers and reduced topsoil erosion by reducing the frequency and need for tillage. Furthermore, PA reduced water use for crop production by only supplementing water for water-stressed plants detected through remote sensors (Zhang et al., 2002).

Initially, satellites and planes were the critical tools for PA to profile fields and make crop management decisions. These systems are costly, prohibitive to many farmers, and cannot provide timely information. The domain of PA moved to use Uncrewed aerial vehicles (UAV) or uncrewed aerial systems (UAS) coupled with remote sensors and image processing as a cost-effective alternative(Tsouros, D. C. et al. 2019). These were used to capture aerial images, which are processed, and analyzed to produce a user-friendly map. The map directs the need-based application of water, nutrients, and chemicals. UAVs are quick and easy to deploy for routine crop surveillance. As many models are battery-powered, running costs are significantly less than for a plane, which reduces the barrier to precision agriculture adoption by many farmers.

Complementary to UAV and UAS, uncrewed ground vehicles (UGV) are locally deployed for specific tasks such as weed detection and removal (Cheein, F. & Carelli, 2013; Maes &

Steppe2019), chemical application (Botta et al., 2022), and harvesting (e.g. Ceres et al. 1998; Nguyen et al., 2013). Gonzalez-de-Soto et al. (2015, 2016) reported that using such ground robots reduces farming annual fuel consumption compared to traditional farm equipment such as tractors, especially since farming robots are often hybrid or battery-powered.

One of the newest applications of robotics in PA is pollination. Demonstrations of aerial pollination systems utilizing UAVs have shown promise but are still in the early stages (e.g. Amador & Hu, 2017; Ma et al., 2013). UGV pollination systems have been successfully demonstrated in fields for crops such as Vanilla (Shaneyfelt et al., 2013) and kiwi vines (Williams et al., 2020) and in greenhouses for crops such as tomatoes (Yuan et al., 2016) and bramble crops (Ohi et al., 2018). Natural pollinators have traditionally provided enough pollination to produce a decent crop yield. However, with natural bee populations in decline(Kevan & Viana, 2003), the pressure for greater yields from the same arable land and farming increasingly occurring in high-tech, controlled environments, a demand for alternative pollination methods has arisen (Nimmo, R. 2022). Bees are reported to perform poorly as pollinators in greenhouse environments. Low UV transmission plastic covers reduce or eliminate the ability of bees to locate flowers. The high temperature and humidity also limit bee activity since they can only fly in a narrow range (10-30 degrees Celsius)(Guerra-Sanz, J. M. 2008). Artificial pollination can replace bees in unsuitable environments while maintaining needed pollination rates using minimal labour.

The first step in developing robotic pollinators is flower detection and location, achieved through remote sensing. The development of digital cameras, using CCD and CMOS sensors, and more powerful computers have greatly expanded the use cases of image-based analysis. Neural network algorithms combined with RGB or hyperspectral camera data have given rise to vegetation indices that can measure soil and plant health, crop growth, and nutrient requirements (Kattenborn et al., 2021). The availability of the algorithms through open–sourced coding

platforms has also contributed to creating image libraries to test new detection and analysis algorithms against their predecessor on equal footing (e.g., Lee C. et al. 2016)

Existing remote sensing systems are based on human vision (RGB), mimicking farmers visually observing their fields. However, flowering plants have co-evolved for millennia to interact with insects whose vision spans the UV-G-B range (Briscoe A.D. & Chittka L., 2001). Pollinating insects such as honey bee (Apis sp.) can distinguish crop species and cultivars based on floral patterning indetectable to human vision (Briscoe, A. D., & Chittka, L.,2001), against a complex background, and while airborne. Briscoe and Chittka (2001) hypothesize that this is due to the greater contrast in the UV-G-B spectrum than in the RGB. The UV-G-B spectrum could be better suited to UAV platforms for flower detection as it would mimic pollinator vision and detect intended plant cues for aerial pollinators. Furthermore, if UV-G-B configured cameras provide images that are easier to process than RGB, this would inform engineers and agriculture service providers of possible directions of the industry.

With this background, this thesis focused on designing, developing, and field testing a Nature Inspired Detector (NID), which takes inspiration from bee vision.

0.1 Statement of objectives

The primary objectives of this research work are:

1. To review the current state of floral spectral reflectance in the UV-G-B range for crop species.
2. To develop and test a compact, lightweight, cost-effective detector inspired by bee vision (NID).
3. To develop a digital image processing program for the NID images that detects flowers of different strawberry cultivars.

4. To test the NID and image processing program on an aerial platform over an outdoor strawberry field.

0.2 Thesis Organisation

The thesis is divided into sections such as Introduction; (CH: 1) Methods; two submitted journal articles :(CH: 2) UV floral reflectance of Agricultural species: A Review and (CH : 3) See as a Bee: UV Sensor for Aerial Strawberry Crop Monitoring; and (CH: 4) General conclusion, which summarizes the conclusions derived from papers (2&3) and suggests further avenues to explore.

CHAPTER 1

OVERALL METHODOLOGY

The following chapter describes the systematic study design and steps to complete this work. Methodologies covered in the article Chapters 3 and 4 are only briefly mentioned with referral to the appropriate section for further detail. Fig. 1.1 depicts the main steps for the completion of this thesis.

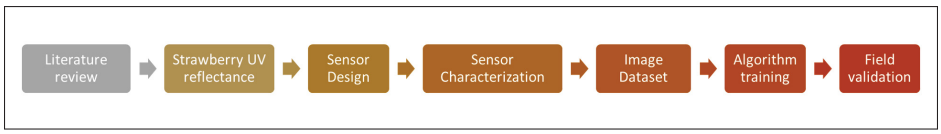

Figure 1.1 Organization of overall methods chapter

1.1 Literature review

A literature review of the UV spectral reflectance of crops was performed using the Scopus scientific database following the eight-step guide for meta-analysis by Hansen C. et al. (2021). The scientific methodology and search criteria are presented in section 2.2. Each article was manually reviewed, which required expertise and knowledge in botany, chemical lab equipment, and camera engineering. In total, 149 papers were used to conduct the meta- analysis for the literature review.

1.2 Strawberry UV reflectance

Rosacea is one of the major families of crops grown in Canada and abroad (Government of Canada, 2021). Despite its great economic importance, little is known about this family's spectral signalling to pollinators. According to anecdotal evidence published by UV photography enthusiasts, *Fragaria Vesca*, *Fragaria vesca L. x viridis*, and *Fragaria viridis* show a UV-reflective bull's eye pattern, more prominently seen on emphFragaria viridis (Rørslett, B.,2006). Almond cultivars, *Prunus dulcis*, have also shown a consistent, distinct peak at 350nm (Chen, B., Jin, Y.,

& Brown, P.,2019). Unlike *Rosacea* orchard species (e.g., apple) some commercial strawberry cultivars are everbearing, flowering throughout the growing season. This, along with its compact habit and flowers held on stocks above the foliage, made it an ideal genus for aerial imagery in this study. *F. x ananassa* 'Seascape' (Fig. 1.1, b.) and 'Fort Laramie' (Fig. 1.1, d.) are commonly recommended commercial everbearing cultivars for central and east coast Canadian provinces (Eric, 2022). Therefore, they were included in this study. *F. x ananassa* 'Hecker' (Fig. 1.1, e.) is an older everbearing cultivar popular with commercial growers for decades before 'Seascape' (Erik, 2022). *F. Vesca* is a woodland strawberry initially kept in French gardens in the 1300s (Hummer, K. E. et al.,2011; Fig 1.1, a.). Today, it is commonly used in genetic studies of *Fragaria sp.* to determine the relatedness of cultivars (Bors, R. H., & Sullivan, J. A.,2005; Marta, A. E. et al.,2004). *F. vesca* was chosen as the comparison specimen to existing spectral data on the floral reflectance database (FReD) to validate lab methodology. Lastly, growers have recently been experimenting with *Fragaria x Comarum palustre* (Marsh Cinquefoil) hybrids resulting in pink or red flowing plants (Mabberley, D. J.,2002). Little is known about how this will affect the visibility of strawberry flowers to insect pollinators. The cultivar *F. ananassa x comarum* 'Berried treasure Red' (Fig. 1.2, c.) was therefore included in this study to explore the spectral properties of such a cross. Specific growing and care methods are presented in section 2.5. I created a spectrogram to assess the ground truth of the cultivar's floral reflectance. I travelled to Laval University with my flowering strawberry plants and collected data over a week. The strawberry cultivars presented in Fig 1.2 were spectrally analyzed using a spectrophotometer at Laval University's biology department. The methodology for the spectral analysis is further described in section 2.5.

1.3 Sensor design

In researching for this thesis proposal, there were no accounts of flower detection using the near UV range (300-400nm) for precision agriculture purposes. Most studies document floral spectral UV reflectance for behavioural interaction studies with pollinators (e.g., Dyer A.G. & Chittka L. 2004; Koski, M. H., & Ashman, T. L.,2015) or species differentiation (e.g., Rieseberg, L. H., &

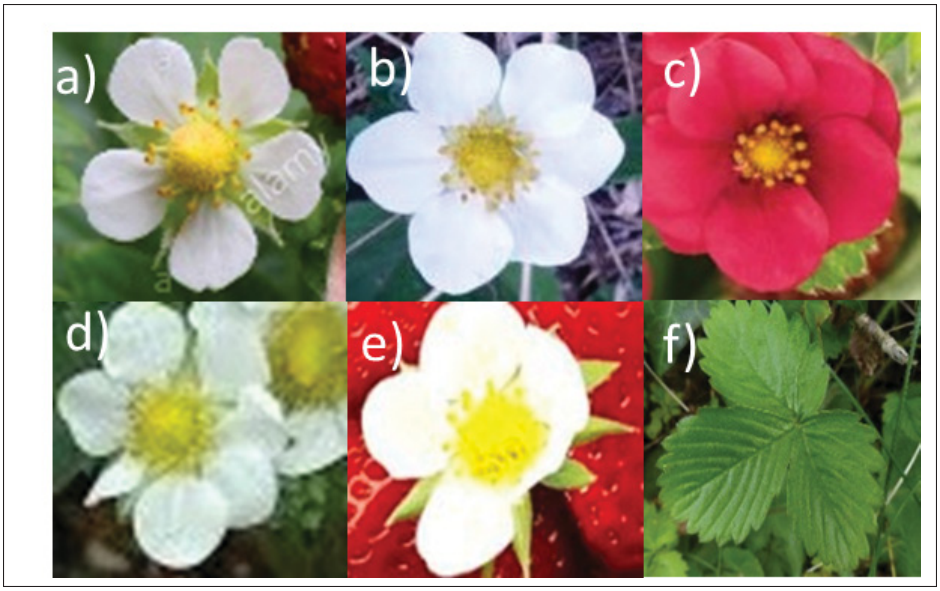

Figure 1.2 RGB images of strawberry cultivars.a) Fragaria vesca b) Fragaria x ananassa "Seascape" c) Fragaria x ananassa (X comarum) "Berried treasure red" d) Fragaria x ananassa "Fort Laramie" e) Fragaia x ananassa "Hecker" f) Fragaria sp. leaf

Schilling, E. E.,1985; Yoshioka, Y. et al. 2005). In agriculture, most remote sensing of crops is in the human vision range, 400-700 nm, and near IR, 700-900nm (Sishodia, R. P., et al. 2020; Wójtowicz, M. et al. 2016). Barriers to exploring UV in remote sensing are likely due to digital UV cameras' size, weight, and price. Therefore, I identified a need for a small, lightweight, cost-effective UV-sensitive camera. The goal was to have a portable and mountable tool for aerial remote sensing. The device in this study needed to be commercially producible, consistent, and sensitive down to 300nm. To mimic the vision range of a bee, a filter, or filter combination, should be used to allow only 300-650nm to reach the sensor. The sensor will henceforth be referred to as the Nature-inspired detector (NID). I determined a CMOS-type sensor would be appropriate to use in the NID as it is sensitive to UV wavelengths, and below 400nm, the sensor is 20% more sensitive than CCD sensors (Bandara, A. M. R. R.,2011, Fig 1.3.). The NID would also need the Bayer filter (Fig 1.4) on the sensor removed, allowing light below 400nm to reach the sensor photodiodes. By removing the Bayer filter, the camera becomes monochrome and will capture images in greyscale. Monochrome images deal with varying lighting conditions

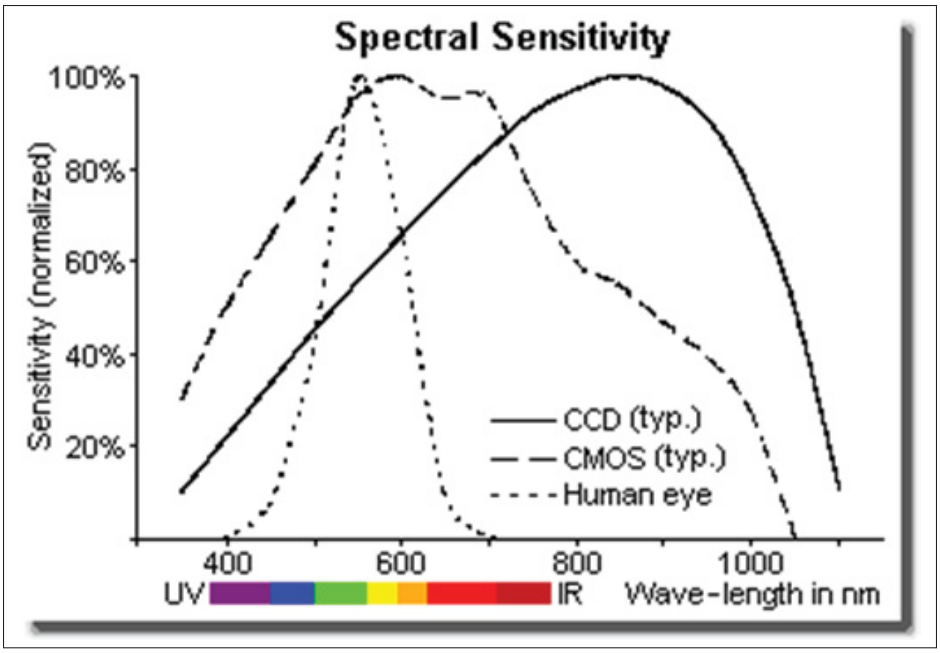

Figure 1.3 Comparison of standard digital sensor's spectral sensitivity (Bandara, et al., 2011).

better than colour images for segmentation (Sridevi, M., & Mala, C.,2012). They also require a third of the memory for storage as compared to RGB. These all work well for outdoor images and on-board image storage and processing. Camera optical windows (or ICF) are generally made from glass, preventing light from passing below 400 nm (MaxMax, 2019), the glass would have to be replaced. I chose Schott WG280 glass which transmits light to 280nm (Fig. 3.3. Optics P.G.,2023). While designing the NID, multiple filter combinations were assessed. The filter combination of BP1 + 330c (Maxmax, 2019) allowed a spectral range of 300-400nm to reach the sensor. However, not enough light reached the sensor in this setup, and images were blurred (e.g. Fig. 1.5). Strawberry flower petals exhibited UV absorbance across cultivars. The remote sensor was changed to a Nature Inspired detector (NID) which shared the same spectral range as a bee pollinator (300-650nm) by using the BP1 filter only. The final model choice and design are presented in section 3.5.1.

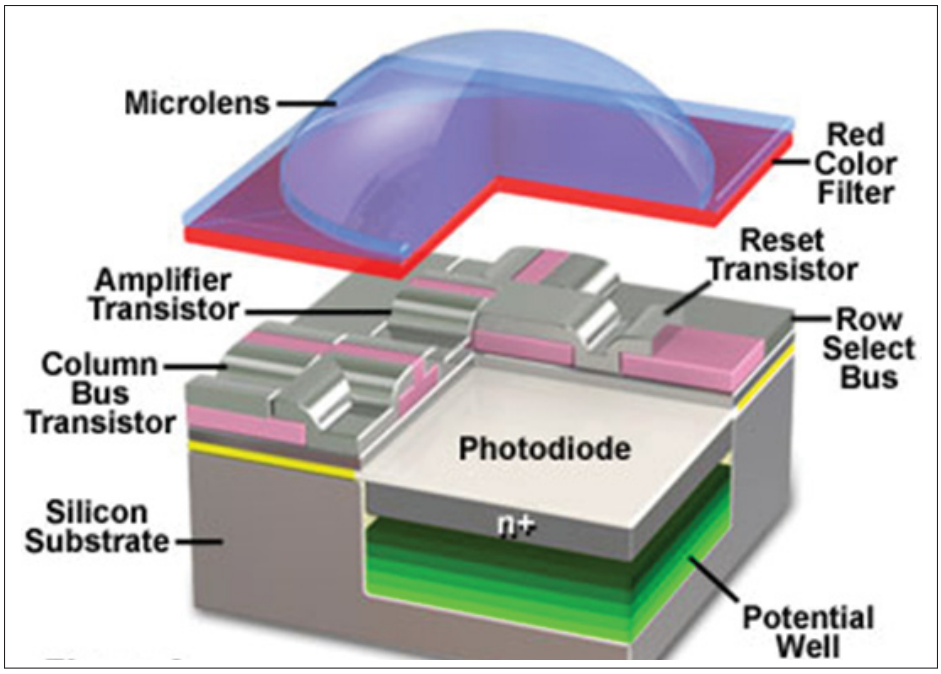

Figure 1.4 Anatomy of a red pixel on the photodiode (MaxMax, 2019).

1.4 Sensor Characterization

In order to establish the NID sensor's response to incoming wavelength, the NID was characterized as described in Garcia et al. (2014; equation 1).

$$\rho = G(n) \tag{1.1}$$

where, ρ is the pixel intensity, G is that sensor's constant, unique to each sensor type, and n is the % reflectance by an object and received on a photoreceptor to produce a signal response. To measure ρ and % reflectance, I created UV reflectance standards following the indications first described by Dyer A.G. et al. (2004). Unlike commercial photography standards, these standards create a more consistent linear response below 400nm. Each reflectance standard was measured with a Perkin Elmer's Lambda 850 UV-VIS spectrophotometer at the University of Laval in Quebec City, Canada. The intercept of the line of best fit produced our % reflectance

Figure 1.5 UV image of Strawberry cultivar using the NID with xNite BP1 and 330c external filters.

values (Fig. 1.6). The UV reflectance standards were photographed with the NID under various solar intensities (8 different days, 55569- 114008 LUX) to measure the rho values captured by the NID sensor. The average of 10 pixels for each standard over the eight days established the rho values. The sensor response curve is presented in section 3.5.2 with further detail pertaining to the methodology.

1.5 Image dataset

Machine learning algorithms require an Image Dataset to train for object detection. The NID system is comprised of the remote sensor and detection algorithm. As most image libraries (containing image datasets of various objects) are comprised of RGB images, I created a new image dataset using the NID camera. Setup parameters are presented in section 3.6 and are depicted below in Fig. 1.7 Images were then augmented to increase the robustness of the dataset (presented in section 3.6), which resulted in 284 NID images.

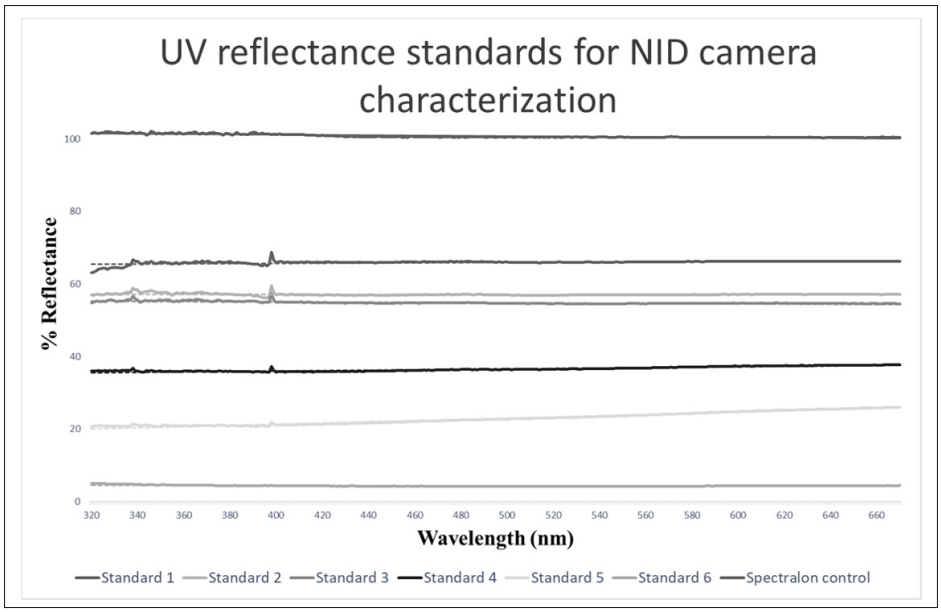

Figure 1.6 UV Reflectance standards measured by spectrophotometer for characterization of NID sensor

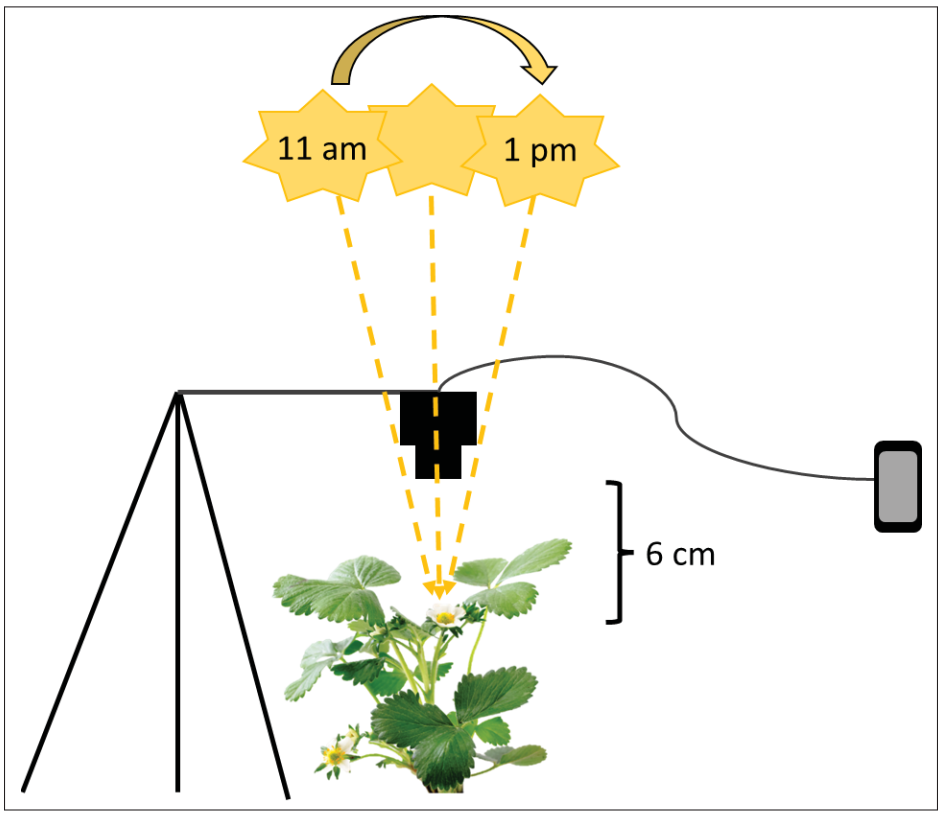

Figure 1.7 NID setup for image dataset generation to train detection algorithm

1.6 Algorithm Training

Simple morphometric algorithms to detect flowers were initially explored, such as Threshold segmentation (Zhou, C. et al. 2020), Canny edge detection (e.g., Jianlun, W. et al. 2016), and Random Forest classification (Zan, X et al. 2020); results were underwhelming. Therefore, more advanced AI algorithms were used to achieve the final detection results. State-of-the-art object detection algorithms, YOLOv5 (Qu, Z. et al. 2022) and Faster R-CNN (Lin, P., & Chen, Y. 2018), were chosen based on their overall performance on MSCOCO2017 and IMAGEnet datasets (Sanchez, S. A., et al. 2020). Their ability to extract complex visual features through hierarchical structures led to better experimental results. Methods for training these two detection algorithms are presented in section 3.6.

1.7 Field Validation

This thesis project required piloting two drone models, DJI M300 and Spiri Mu, for field testing the NID system. The pilot requires a Canadian advanced Drone Pilot license to fly the M300 and Mu. Throughout this degree, I passed the Basic and advanced online Drone pilot certification exams and the in-person flight review for Advanced operations. I also completed the NSERC-funded CREATE Uninhabited aircraft systems Training, Innovation and Leadership Initiative (UTILI) led by Carleton University, the University of Ottawa, Queen's University, L'École de technologie supérieure (ÉTS), Université de Sherbrooke, and Université du Québec en Outaouais (UQO). This program consisted of a semester-long course and a three-month internship with a drone development company, Spiri Robotics. The initial scope of this thesis was to field test the NID system in greenhouse conditions and outdoors. However, the COVID-19 pandemic prevented visitation to farms for field testing. It was necessary to re-create outdoor strawberry field conditions in a fallow field in Ile Perrot, Qc (2021; Fig 1.8).

Row spacing followed the Ontario Ministry of Agriculture guidelines for strawberry cultivation; 0.2m between plants, 1.2m between rows (The Ontario Ministry of Agriculture, Food and Rural Affairs, OMAFRA, 2016). Bare root plants were potted with a 2:2:1 ratio of acidic potting soil,

Figure 1.8 Custom field setup In Ile Perrot, Qc. during lockdown.

shrimp compost and sand in 7.5L containers. Plants were fertilized bi-monthly with 15-30-15 liquid feed to promote flowering. Flights were conducted with the Spiri Mu (Fig 1.9) and DJI M300 (Fig 1.10) drones at 3 and 5 m. Images were captured at 1080p. In post-processing, the flower resolution was too low for accurate results; therefore, a second field test was performed post-pandemic over a commercial strawberry field near Princeville, Qc. These results were used and presented in section 3.9.

Figure 1.9 Spiri Mu Quadcopter UAV used in initial and final field validation trials. A) NID sensor mounted with custom 3D printed parts. B) Extended legs to account for NID sensor.

Figure 1.10 DJI M300 quadcopter UAV using in initial field trials during lockdown

CHAPTER 2

UV REFLECTANCE IN CROP REMOTE SENSING: ASSESSING THE CURRENT STATE OF KNOWLEDGE AND EXTENDING RESEARCH WITH STRAWBERRY CULTIVARS

2.1 Contribution from other Authors

David St-Onge and Robert Hausler provided editorial notes for final journal submission.

Megan Heath[1] , David St-Onge[1] , Robert Hausler[1]

[1] Département de Génie Mécanique, École de Technologie Supérieure, École de technologie supérieure, Montreal, Quebec, Canada
1100 Notre-Dame Ouest, Montréal, Québec, Canada H3C 1K3

Article submitted for review « environmental stream » in March 2023.

2.2 Abstract

Spectral reflectance is a standard parameter used in precision agriculture through remote sensing. The colour produced when light is reflected from a plant's surface can be used to indicate health (VIS-IR)or to direct visiting pollinators(Near-UV). However, crop species are a minority of plants presented in UV spectral reflectance studies, which contain vital information for plant-pollinator interaction. This literature review discusses crop UV-reflectance, identifies gaps in the literature and contributes new data using strawberry cultivars. Results showed that most crop spectral reflectance studies used lab-based methodologies, presented wide spectral ranges (Near UV to IR), and the plant family distribution mirrored global food market trends. The spectral comparison of human white flowering strawberry cultivars indicated visual differences for pollinators in the Near UV and Blue ranges. Variation in pollinator visibility among strawberry cultivars indicates a need to consider UV spectral reflectance when creating new breeding lines and managing pollinator preferences in agricultural fields.

Introduction

Precision agriculture (PA) incorporates modern technology with traditional farming principles to manage fields with minimal inputs and human resources. Remote sensing, based on electromagnetic radiation, is an integral tool for modern PA (Wójtowicz M. et al.,2016; Xue, J., & Su, B., 2017). The data from passive remote sensors, capturing electromagnetic reflectance from vegetal surfaces, is routinely used to generate field maps. Vegetation indices (VI) are then applied to characterize biophysical features such as water and nutrient stress, presence of

infection/disease, or overall growth of crops(Zhang & Kovacs, 2012; Liu C. et al., 2016). The principal spectral regions for agricultural remote sensing are (i) ultraviolet (UV), (ii) visible, and (iii) near-infrared (IR) (Xue, J., & Su, B. 2017).

2.2.1 Flower Patterns in UV

The colours and patterns of flowers are diverse and have been the focus of pollinator interaction studies since Darwin (1876). Unlike many foraging predators, pollinating species have receptors for UV (Briscoe, A. D., & Chittka, L.,2001). Plants have developed UV floral patterns to attract beneficial insects visually but remain cryptic to foraging species. Compounds that absorb or reflect radiation are arranged in patterns on reproductive structures, such as anthers and petals, to signal landing and feeding locations and differentiate plants from con-specifics, even to the cultivar level (Yoshioka, Y. et al., 2005). The size, shape, and contrast of this patterning can affect how visible one plant is from its con-specifics, especially from the air. Spaethe J. et al. (2001) found that floral signalling strategies may respond to the perceptual constraints of their pollinators. Bumblebees favoured high colour contrast on the floral surface for large flowers (e.g., UV pattern) but only favoured high contrast with green foliage for small flowers. Optimal foraging strategies resulted due to more accurate floral recognition while in flight. A typical signalling pattern of large flowers is the "bullseye" pattern, where flowers consist of UV-absorbing centers and UV-reflecting peripheries. Previous studies have shown that bees make their first antennae contact with the UV-absorbing part and that untrained bees preferentially visit bullseye-patterned flowers (e.g., Koski Ashman, 2014; Papiorek et al., 2016).

2.2.2 Factors affecting crop visibility to pollinators

However, this pattern becomes less visible under the physical conditions of greenhouses that commonly employ UV-blocking coverings (Morandin, L. A. et al. 2002). In a study by Morandin et al. (2001), four types of polyethylene greenhouse coverings, varying in their UV transmittance, found that bees made twice as many foraging trips under low UV transmittance plastics. Furthermore, 136 percent more bees remained within the greenhouse after ten days,

drastically affecting operation costs and crop production. Bee pollination of crops results in heavier, more uniform crops, which fetch a higher market value. Therefore, hives are often supplemented in agricultural settings (e.g. Klatt, B. K. et al. 2014). Another factor for commercial growers to consider is the genetic component of UV patterns when breeding new cultivars. Brock M. T. et al. (2016) showed that UV patterning varied greatly among Brassica rapa genotypes and that insects preferred flowers with UV patterns over those without patterns, such as their wild relatives. Moyers et al. (2017) found that the UV pattern of sunflowers could be modified without affecting flower head size based on the mapped genetic architecture. Flower head size is a critical trait for breeding this crop and could have unintended effects on pollinator–flower interactions. Breeders need to consider the genetic architecture of a crop when creating new cultivars. Research supports that colour patterning in various crop families varies significantly with heredity (e.g., Mangelsdorf, A. J., & East, E. M.,1927; Henz, A. et al., 2015; Muchhala, N. et al., 2014). However, few studies have explored the use of UV floral reflectance of plants, even fewer for crops specifically. Spectral reflectance studies have reported down to 300 nm, but most species in reflectance databases (e.g., FReD) are native species, not crop species (Arnold S. et al. 2008).

2.2.3 UV floral reflectance of Rosacea crops

The Rosacea family includes orchard and berry crops such as apples, cherries, raspberries, and strawberries. It is one of the four main crop families grown commercially in greenhouses worldwide (Guerra-Sanz, J. M. 2008). Members of the Rosacea plant family, including blackberry and almond cultivars, have shown consistent and distinct peaks in the near UV range (Gyan, K.Y.& Woodell, S.R.J., 1987; Chen, B. et al. 2019). These peaks suggest that UV patterning may play a role in pollinator signalling within the family. Strawberries are a highly selectively bred crop and are prominently grown worldwide; under greenhouse and field conditions. In 2021 global greenhouse production was a 34.8 billion dollar industry, with North America holding the largest market share, 32.8 percent (Precedence Research, 2022). Total production was 41 percent vegetable and 25.4 percent fruit (Forbes, 2022), with tomatoes and strawberries

as the leading crops in each category. When considering field production, Rosacea crops represented the majority of global fruit production in 2021 (strawberries representing 75.4 percent of berry crops), competing with the Musaceae (bananas and plantains), Rutaceae (citrus), and Cucurbitacea (melon) families, as depicted in Fig 1. (Statista, 2023). However, research has yet to explore the UV floral reflectance of strawberry cultivars. Although most strawberry flowers appear white to human eyes, Ceuppens et al. (2015) observed dissimilar pollination of two related strawberry varieties when cultivated together. The role of volatile floral substances was explored to account for this phenomenon but yielded inconclusive results. Therefore, floral patterning differences are potentially a factor here. There have yet to be any literary reviews of UV floral reflection of crop species. This study documents the state of Floral UV-reflectance of crops in scientific literature and expands upon it with strawberry cultivars.

2.3 UV crop reflectance: what we know and what we need

Methodology

In this literature review, we analyzed scientific articles studying the UV-reflectance of crops. We searched the electronic database Scopus (1969-2020) for the following search strings: UV* OR ultraviolet AND camera AND/OR "Spectral reflectance" AND "flo*" AND/OR "crop*" AND/OR "plant*". In addition, searches were limited to the English language, publication in a journal or conference proceeding, and fell within the categories <agriculture>, <botany>, AND/OR <environmental sciences>. A total of 1013 articles met the search criteria and were screened for crop species and spectral reflectance under 400 nm using a single reviewer. We excluded 1593 papers that dealt with the spectral reflectance of compounds derived from plants in chemical isolation or studied UV spectral fluorescence rather than reflectance from this review. UV Reflectance measures a reflected wavelength in the near UV range (300-400 nm), often used by flowering plants for pollinator signalling. In contrast, UV fluorescence is a visible emission of wavelengths due to a substance or pigment's absorbance of UV radiation. Until recently, the terms were used interchangeably in literature; therefore, we carefully examined the

methodologies employed. In total, 170 papers related to botanical plants, of which 149 covered spectral reflectances below 400 nm in some capacity. When filtered for agriculturally relevant species, 52 records remained from 29 families and 73 crop species, as listed in Table 1.

Table 2.1 Major characteristics of studies included in the meta-analysis from 1969-2020

Family	Species	Common name	Plant part	Range	Instrument type	Reference
Family: Altingiaceae						
	Liquidambar styraciflua	American Sweet-gum tree	leaf	280 - 400 nm	Spectroradiometer	Yang X., et al. 1995
Family: Amaranthaceae						
	Beta vulgaris	Beet	stock	300-800 nm	Spectrometer	Peters R.D. & Noble S.D., 2014
	Spinacia oleracea	Spinach	leaf	300-800 nm	Spectrometer	Peters R.D. & Noble S.D., 2014
Family: Amaryllidaceae						
	Allium schoenoprasum	Chive	flower	300-700 nm	Spectrophotometer	Chittka L., et al. 1994
				350-400 nm	Film camera	Utech F.H. &Kawano S., 1975
Family: Anacardiaceae						

	Mangifera indica	Mango	fruit	360 nm	Digital camera	Patel K.K., et al. 2019
Family:Apiaceae						
	Daucus carota	Carrot	root	300-800 nm	Spectrometer	Peters R.D. & Noble S.D., 2014
Family:Asteraceae						
	Carthamus tinctorius	Safflower	stamen	200– 700 nm	Spectrophotometer	Varliklioz Er S., et al. 2017
	Cichorium intybus	Chicoy	flower	300-700 nm	Spectrophotometer	Chittka L., et al. 1994
				350-400 nm	Film camera	Utech F.H. &Kawano S., 1975
	Helianthus annus	Sunflower	flower	320 and 380 nm	Digital camera	Moyers B.T., et al. 2017
				200-400 nm	TV camera	Takiguchi Y., et al. 1998
Family:Betulaceae						

	Betula sp.	Alder tree	wood	200-400 nm	Digital camera	Hirvonen T., et al. 2014
Family: Brasicaceae						
	Brassica napus	Rapeseed	leaf	300-700 nm	Spectrophotometer	Cen Y.-P. & Bornman J.F., 1993
	Brassica nigra	Mustard	leaf	190-890 nm	Spectrometer	Ngo V.-D., et al. 2013
	Brassica oleracea	Broccoli	flower	350-400 nm	Film camera	Utech F.H. &Kawano S., 1975
	Brassica oleracea	Red cabbage	leaf	300-800 nm	Spectrometer	Peters R.D. & Noble S.D., 2014
	Brassica rapa	Broccoli rabe	leaf	190-890 nm	Spectrometer	Ngo V.-D., et al. 2013
Family:Cucurbitaceae						
	Cucurbita pepo	Pumpkin	leaf	200-780 nm	Digital monochrome camera	Liu H., et al. 2018

				200-500 nm	Digital camera	Liu H., et al. 2017
	Cucurbita pepo	Zucchini	leaf	195 to 1122 nm	Spectrometer	Rivera-Romero C.A., et al.2020
	Lagenaria sicer-aria	Chinese bottle gourd	leaf	200-780 nm	Digital monochrome camera	Liu H., et al. 2018
				200-500 nm	Digital camera	Liu H., et al. 2017
Family:Ericaceae						
	Vaccinium cyanococcus	Blueberry	leaf/fruit	200-2500 nm	Spectrophotometer	Yang C. & Lee W.S., 2011
	Vaccinium vitis-idaea	Lingonberry	flower	300-700 nm	Spectrophotometer	Chittka L., et al. 1994
	Vaccinium myr-tillus	Bilberry	flower	300-700 nm	Spectrophotometer	Chittka L., et al. 1994
Family:Eucommiaceae						
	Eucommia ul-moides	Chinese medici-nal herb/tree	bark/leaf	190-750 nm	Spectrophotometer	Wang C.-Y., et al. 2021
Family:Fabaceae						

	Glycine max	Soy bean	seed	300–2500 nm	Spectroscopy	Ogruc Ildiz G., et al. 2020
	Glycine max	Soy bean	leaf	325–1075 nm	Spectroradiometer	Kovar M., et al. 2019
				350-2500 nm	Spectroradiometer	Koger C.H., et al. 2004
				350-2500 nm	Spectroradiometer	Koger C.H., et al. 2004
	Lupinus poly-phyllus	Lupin (fodder crop)	leaf	207-407 nm	Spectroradiometer	Jan S., et al. 2016
	Medicago sativa	Alfalfa	flower	300-700 nm	Spectrophotometer	Chittka L., et al. 1994
Family:Fagaceae						
	Quercus rubra	Red oak tree	leaf	280 to 400 nm	Spectroradiometer	Yang X., et al. 1995
	Quercus velutina	Black oak tree	leaf	280 to 400 nm	Spectroradiometer	Yang X., et al. 1995
	Quercus alba	White oak tree	leaf	280 to 400 nm	Spectroradiometer	Yang X., et al. 1995

	Quereus macrocarpa	Burr oak tree	flower	350-400 nm	Film camera	Utech F.H. &Kawano S., 1975
Family:Iridaceae						
	Crocus sativus	Saffron	stamen	200– 700 nm	Spectrophotometer	Varliklioz Er S., et al. 2017
Family:Juglandaceae						
	Juglans regia	Walnut tree	leaf	200 to 800 nm	spectrometer	Mirza A.U., et al. 2019
	Carya illinoinensis	Pecan	leaf	280 to 760 nm	Spectroradiometer	Qi Y., et al. 2003
	Carya tomentosa	Mockernut hickory	leaf	280 to 400 nm	Spectroradiometer	Yang X., et al. 1995
Family:Laminaceae						
	Origanum vulgare	Oregano	flower	300-700 nm	Spectrophotometer	Chittka L., et al. 1994
Family:Malvaceae						
	Abelmoschus esculentus	Okra	root	190–1400 nm	Spectrophotometer	Sharma N., et al. 2018

	Gossypium arboreum	Cotton	leaf	250-2000 nm	Spectrophotometer	Thomasson J.A. & Sui R., 2009
Family:Musaceae						
	Musa (AAB) simmonds	Banana	fruit	270-1000 nm	Digital camera	Santoyo-Mora M., et al. 2019
Family:Onagraceae						
	Fuchsia excorticata	Fuchsia berry	fruit	300-400 nm	Digital camera	Lee W.G., et al. 1990
Family:Passifloraceae						
	Passiflora edulis	Passionfruit	leaf	200-780nm	Digital monochrome camera	Liu H., et al. 2018
				200-500nm	Digital camera	Liu H., et al. 2017
Family:Pinaceae						
	Picea abies	Spruce tree	wood	200-400nm	Digital camera	Hirvonen T., et al. 2014
	Pinus sylvestris	Pine tree	wood	200-400nm	Digital camera	Hirvonen T., et al. 2014

Family:Poaceae						
	Avena strigosa	Oat	seed	365-970nm	VideometerLab4® instrument	França-Silva F., et al. 2020
	Hordeum vulgare	Barley	grain	250–430 nm	hyperspectral imaging line scanner	Brugger A. et al, 2021
	Hordeum vulgare	Barley	leaf	240–500 nm	UV line scanner	Brugger A., et al. 2019
				300-800nm	Spectroradiometer	Klem K., et al. 2012
	Oryza sativa	Rice	leaf	350-1050 nm	Spectroradiometer	Wang X., et al. 2003
	Triticum aestivum	Wheat	grain	200-2500 nm	Spectroradiometer	Balcerowska G., et al. 2009
				200-2500 nm	Spectroradiometer	Siuda R., et al. 2006
	Triticum aestivum	Wheat	leaf	300-700 nm	Spectroradiometer	Schröder M.L., et al. 2014
				325– 1075 nm	Spectroradiometer	Ray S.S., et al. 2007

				350-1050nm	Spectroradiometer	Prasad B., et al. 2007
	Zea mays	Corn	seed	200-1100nm	Spectrometer	Smeesters L., et al. 2016
	Zea mays	Corn	stock	250-750 nm	Spectroradiometer	Li X., et al. 2016
	Zea mays	Corn	leaf	300-700 nm	Spectroradiometer	Schröder M.L., et al. 2014
Family:Rhamnaceae						
	Ziziphus jujuba	Jujube	leaf	300-900 nm	Spectrophotometer	Yang W., et al. 2014
Family:Rosaceae						
	Fragaria x ananassa	Strawberry	flower	350-400 nm	Film camera	Utech F.H. &Kawano S., 1975
	Fragaria x ananasa	Strawberry	fruit	374–1020 nm	Spectrophotometer	Weng S., et al. 2020
	Fragaria vesca	Wild Strawberry	flower	300-700 nm	Spectrophotometer	Chittka L., et al. 1994

	Malus pumila	Apple	leaf	200 to 800 nm	spectrometer	Mirza A.U., et al. 2019
				300–900 nm	Spectrometer	Zhang Y., et al. 2015
	Malus pumila	Apple	fruit	350-800 nm	Spectrophotometer	Venturello A., et al. 2012
				300–800 nm	Spectrophotometer	Merzlyak M.N., et al. 2005
	Prunus avium	Sweet cherry	flower	300-700 nm	Spectrophotometer	Chittka L., et al. 1994
	Prunus cerasus	Sour cherry	fruit	350-1050 nm	Spectrophotometer	Shrestha B.P., et al. 2004
	Prunus persica	Peach	leaf	200-780 nm	Digital monochrome camera	Liu H., et al. 2018
				200-500 nm	Digital camera	Liu H., et al. 2017
				350-2500 nm	Spectrometer	Minghua Z., et al. 2008

	Prunus spinosa	Blackthorn	flower	300-700 nm	Spectrophotometer	Chittka L., et al. 1994
	Rubus idaeus	Red raspberry	leaf	330-1100 nm	Spectrophotometer	Feldhake C.M., 2002
	Rubus illecebrosus	Balloon berry	flower	350-400 nm	Film camera	Utech F.H. &Kawano S., 1975
	Rubus occidentalis	Black raspberry	leaf	330-1100 nm	Spectrophotometer	Feldhake C.M., 2002
Family:Sapindaceae						
	Acer saccharum	Sugar maple	leaf	280 to 400 nm	Spectroradiometer	Yang X., et al. 1995
	Acer platanoides	Norway maple tree	leaf	280 to 400 nm	Spectroradiometer	Yang X., et al. 1995
Family:Solanaceae						
	Capsicum annuum	Bell pepper	leaf	200-780 nm	Digital monochrome camera	Liu H., et al. 2018
				200-500 nm	Digital camera	Liu H., et al. 2017

	Solanum lycoper-sicon	Tomato	leaf	200-2500 nm	Spectrophotometer	Jones C.D., et al. 2010
				200-780 nm	Digital monochrome camera	Liu H., et al. 2018
				200-500 nm	Digital camera	Liu H., et al. 2017
				325-1075nm	Spectroradiometer	Cui D., et al. 2009
	Solanum tubero-sum	Potato	leaf	300-700 nm	Spectrophotometer	Schröder M.L., et al. 2014
	Solanum tubero-sum	Potato	tuber/root	300-420 nm	Digital camera	Al-Mallahi A., et al. 2010
Family:Theaceae						
	Camellia sinen-sis	Tea tree	leaf	300 to 700 nm	Spectrometer	Bian L., et al. 2020
Family:Vitaceae						
	Vitis vinifera	Grape	leaf	380–1000 nm	Digital Hyperspectral camera	Debnath S., et al. 2021

				200-780 nm	Digital monochrome camera	Liu H., et al. 2018
				200-500 nm	Digital camera	Liu H., et al. 2017
Family:Zingiberaceae						
	Curcuma longa	Turmeric	root	200– 700 nm	Spectrophotometer	Varliklioz Er S., et al. 2017

2.3.1 Metrics

Articles meeting the above criteria had the following parameters noted: instrument model used, the spectral range for measurements, floral part and species analyzed, and year of publication.

Instrument models were grouped into 4 categories: Camera, Videometer, spectrometer/spectro-radiometer, and spectrophotometer. Cameras were defined as self-contained, image-recording devices which relied on an external light source. This included video, monochrome, multi-spectral, and hyper-spectral cameras which employed CMOS or CCD sensors, as well as UV film cameras. Spectrometer and spectroradiometer were grouped together as the terms are often used interchangeably. A spectrometer measures the reflectance spectrum of an object or substance. Its sensor array can separate out the light received at each wavelength and generate an amplitude graph of the incoming signal. A spectroradiometer can also take calibrated readings of power, intensity, and radiance of the incoming signal at each wavelength (International Light Technologies Inc.,2019). On the other hand, Spectrophotometers measure the light absorption or transmission of a sample. A reflectance curve can then be generated from the absorption and transmission measurements using Kirchoff's law (Spectrecology,2021). Videometer was its own category as it utilizes an integrating sphere with a light-emitting diode, similar to a spectrometer; however, the sensor captures a pixelated image of an object at each wavelength (Carstensen, J. M.,2022).

For all instruments, spectral ranges were binned according to the following nanometer (nm) ranges: near UV (<300-380nm), Blue (381-520nm), Green (521-625nm), red/ IR (>625nm) in accordance with the international society for optics and photonics (Malacara, D., 2011).

Floral parts analyzed were grouped into 5 categories: flower, stem, leaf, fruit, and root. Flower included the anther, stamen, petal, and sepal elements of a plant's reproductive structure. The stem encompassed dermal (cork & bark) , vascular (xylem & phloem), and ground tissues (parenchyma, collenchyma,& sclerenchyma). Fruit encompassed seed and/or ripened ovary of a flowering plant. Root included tubers as well as roots themselves. Leaf category contained

upper and lower sides of leaves. The species studied were divided by plant family to assess trends in the literature.

Trends in research over time were assessed by cross-referencing the above parameters with the publication year.

2.4 Results

2.4.1 Instrumentation

Most methodologies consisted of lab bench setups due to the size, weight, and equipment cost (e.g., Spectrophotometer). Of the data collection methods in Table 1, less than a third (31.7%) used cameras. UV Film represented 20% of data collected and occurred before 1980. After 1980 digital data collection using cameras became standard. The average cost of the cameras was $772.50 CAN and varied in weight from 50g to 2.75 kg, averaging 302g across all species recorded. Of note: no studies performed aerial remote sensing of UV reflectance. Fig. 2.1 depicts the trends in instrumentation. Spectrometers/Spectroradiometers and Spectrophotometers comprise the bulk of collection methods (36.8% and 27.4%, respectively) and have occurred consistently since the early 1990s. These are lab-based, costly devices, often shared with other departments, such as chemistry. They allowed for quantitative analysis using spectrograms compared to qualitative analysis with film cameras, as seen in Utech F.H. & Kawano S. (1975).

2.4.2 Spectral range

Though all publications in this study had to include the near UV range (<300-380nm), many also presented visible and near IR spectrums. Cameras presented narrower ranges (Near Uv to blue) more often than any other instrument category, followed by Spectrometer /Spectrophotometers (Fig 2.1). We attribute this disparity to the nature of the instrumentation chosen for the study. Digital cameras have a sensor that is more sensitive to Red and Near IR wavelengths. Therefore, a narrow range (usually Near UV to blue) must be captured using specialized lenses and filters to

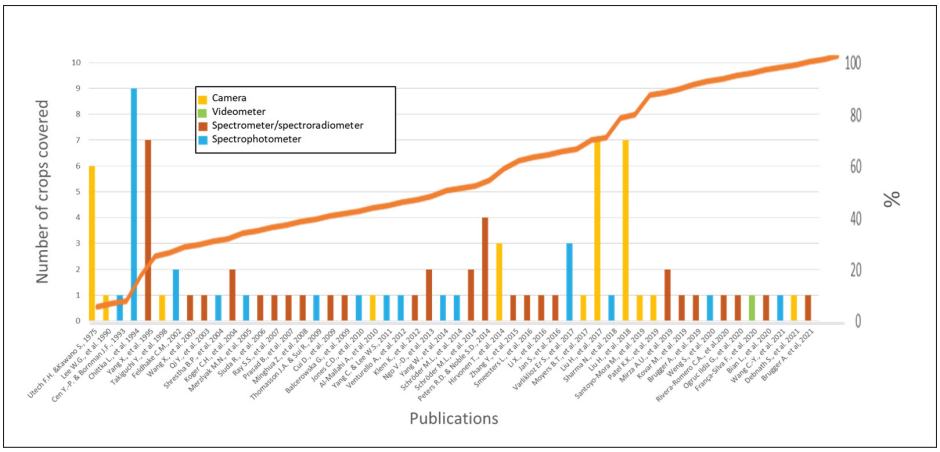

Figure 2.1 Trends in UV reflectance. Publications from meta-analysis ranging from 1960 to 2021 for crop UV spectral reflectance

capture UV imagery. Comparatively, Spectrophotometers, Spectrometers, Spectroradiometers, and Videometers can capture data to the nm level without such interference. Authors usually capture complete spectral ranges with these devices, even if the publication only interests a particular region.

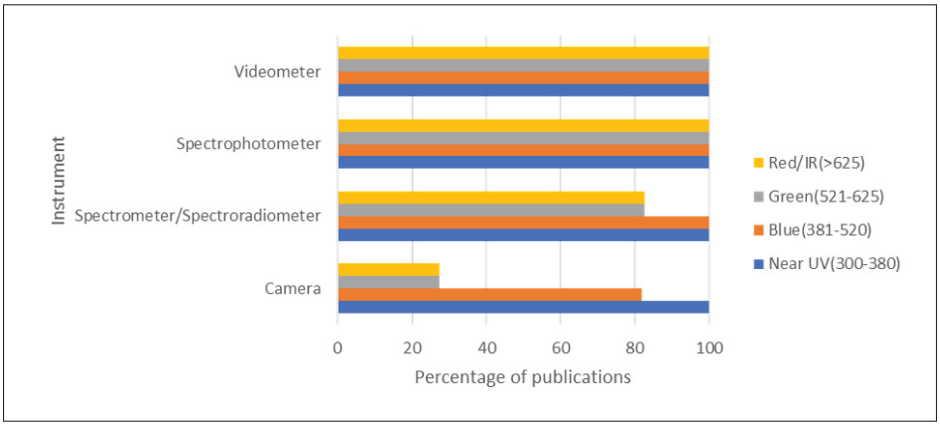

Figure 2.2 Spectral ranges presented in Crop UV reflectance literature

2.4.3 Species and floral parts

As previously stated, 73 crop species from 29 families were included in this meta-analysis, as listed in Table 1. Compared to the global production of fruits and vegetables in Fig. 2.3, we see an overlap in crop family representation from our metanalysis in Fig. 2.4. Four of the top five families in our literature review (Rosacea, Solanaceae, Fabaceae, and Brassicaceae) overlapped with global production's largest fruit and vegetable families in 2021. The Rosaecea family was the largest in global fruit production, whereas Solanaceae, Fabaceae/ Leguminaceae and Brassicaceae were the top three vegetable-producing families globally in 2021, respectively. The above four families comprised 36.8% of the publications in our meta-analysis. The disproportional representation of the above families in our review supports that research decisions for crop species follow market trends.

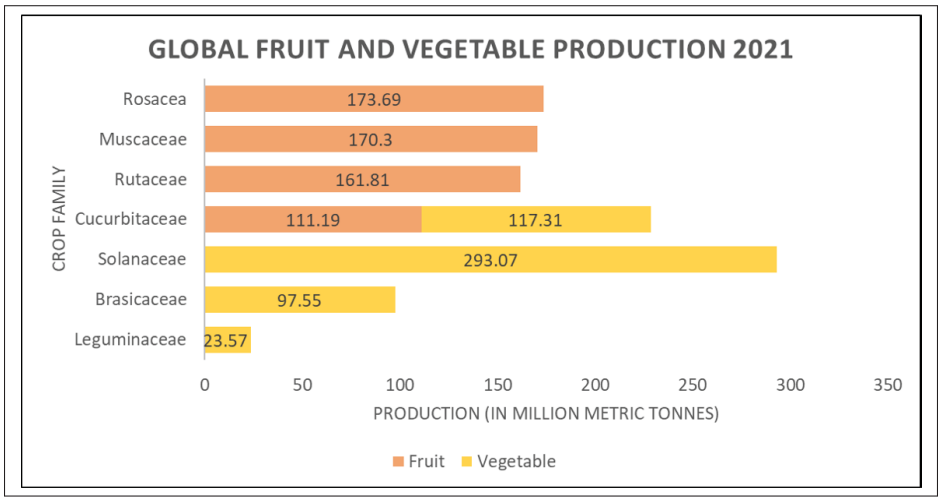

Figure 2.3 Global Fruit and Vegetable Production 2021

When considering crops, choosing which floral part to research indicates the research focus. Fig. 2.5 illustrates the distribution of research across floral parts for our meta-analysis.

Publications focused on stems and roots (6.4 and 4.3%, respectively) assessed the quality of a given crop, e.g., lumber or tubers. Papers containing leaf reflectance represented most of our study's published research (55.7%). These papers assessed growth rate, plant stress or nutritional deficiencies. Papers presenting the spectral reflectance of fruits (14.9%) had contents that varied

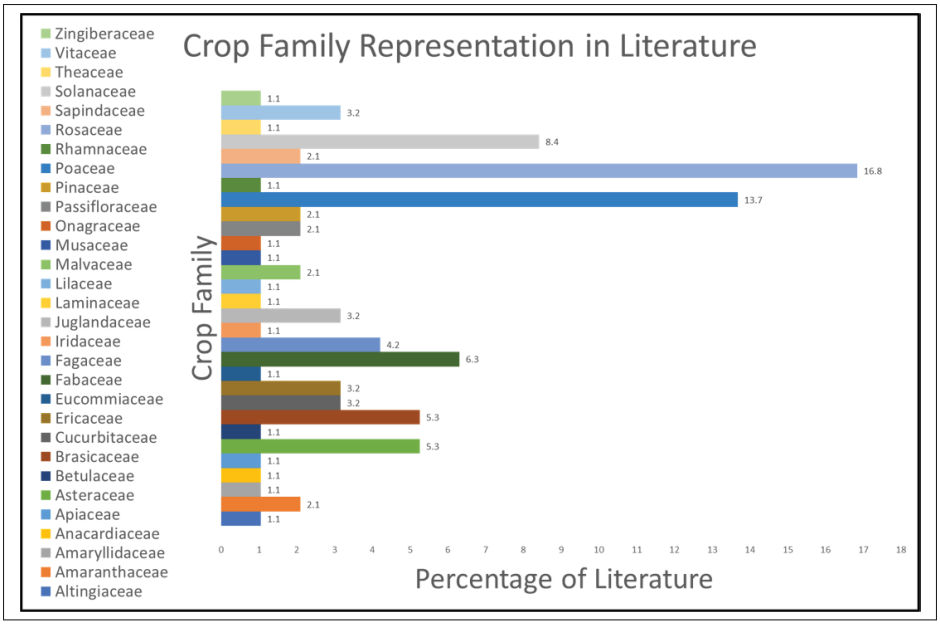

Figure 2.4 Crop family representation in UV reflectance literature from 1969 to 2021

the most. Spectral reflectance was used to assess fruit ripeness and flavour quality, detect disease, and train detection algorithms for remote sensors. Papers analyzing flowers (20%) comprised two categories: pollinator-plant interaction and remote flower detection. However, over a third of all the flowers documented (31.57%, Table 1) were captured on UV film (Utech F.H. & Kawano S., 1975). UV film, just like any camera film, is prone to human error during development, which can make the reported reflectance pattern or intensity questionable. Utech, F. H., & Kawano, S. (1975) reported a pattern of central petal absorption and UV reflecting anthers for two Rosaceae species Fragaria x ananassa 'Duchesne' and Rubus illecebrosus' Focke.' However, spectrophotometric readings of wild Fragria did not indicate this reflectance. As there is a lack of data on strawberry (Fragaia) flower reflectance, one of the most significant contributors to the Rosaceae family's global dominance in the fruit industry, we assessed the spectral reflectance of a variety of strawberry cultivars both quantitatively using a spectrophotometer and qualitatively using a UV sensitive camera.

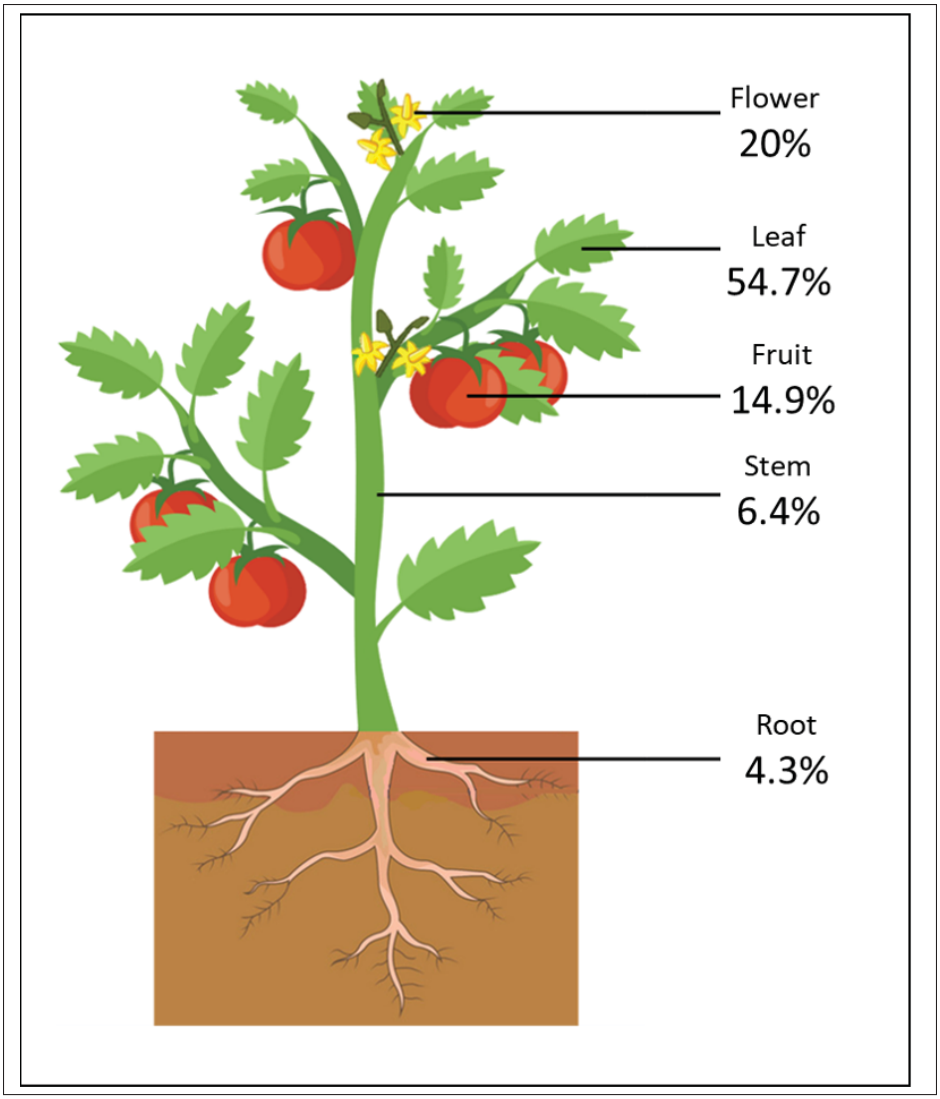

Figure 2.5 Floral parts spectrally analyzed in our literature meta-analysis

2.5 Spectral analysis of Strawberry cultivars

The Rosacea family contains many orchard species, such as apples and cherries, and berry species, such as strawberries and raspberries. Crops in the Rosacea family share similar floral phenotypic traits, such as five radially symmetrical sepals and petals, spirally arranged stamens, and a cup-like structure at the flower base known as a hypanthium (Heywood, V.H. et al., 2007). Due to their visual floral similarity, remote sensing and pollinator vision studies involving these

crops tend to extend findings to the whole family (e.g., Dias P.A. et al., 2018; Eeraerts, M. et al., 2020). However, only some studies have investigated the actual spectral reflectance of Rosacea flowers.

2.5.1 Methodology

As our literature review revealed a need for floral UV spectral reflectance measures for widely cultivated species, such as strawberries, we performed measurements to add them to the global floral reflectance database. We present spectral differences between strawberry cultivars resultant from our measures below.

2.5.1.1 Plants

Bare root plants of day-neutral *Fragaria ananassa sp.* cultivars ("Fort Laramie", "Hecker", "Seascape"), wild ancestor *Fragaria vesca*, and Asian *Fragaria ananassa x F. comarium* hybrid ("Berried Treasure Red") were purchased from ©2020 Vesey Seeds. Plants were potted with a 2:2:1 ratio of acidic potting soil, shrimp compost, and sand in 7.5L containers and fertilized bi-monthly with 15-30-15 liquid feed. We removed flowers for imaging within 12 hours of opening and imaged the petal(P), anther(A), sepal(S) and upper leaf (L) from each flower. All plants used in this study were in good health and grown outdoors under natural light.

2.5.1.2 Reflectance spectra of Fragaria sp. flowers

We collected spectral reflectance measurements with a Perkin Elmer's Lambda 850 UV-VIS spectrometer at the University of Laval in Quebec City, Canada. All flowers imaged were within 12 hours of first flowering and were intact. Each flower comprised three 'samples': full flower upper side, petal only, and central anther and stamen disk only. We imaged the leaves of each cultivar on the upper and lower surfaces. At least two flowers or leaves per cultivar plant were measured. The Spectrophotometer was calibrated using Spectralon as suggested by the manufacturer. The measurement interval was set to 1nm with scans conducted over the

200-700nm range and repeated thrice per sample. Results were exported as an Excel spreadsheet of % reflectance values.

2.5.1.3 Quantifying contrast of floral parts

We quantified the visibility (△S)of strawberry flowers to pollinators using the Normalized Segment Classification (NSC) vision model (Rodríguez-Gironés, M. A., & Telles, F. J., 2020). Unlike previous segment classification models, the NSC model is 1) species independent and 2) considers brightness in its calculation. The model calculates a value (△S) based on the Euclidean distance between two spectrogram curves, indicating their contrast. The larger the number, the greater the contrast.

2.5.2 Results and Discussion

We present the spectrograms for Fragaria vesca (Fig 2.6a), the four Fragaria x ananassa cultivars (Fig 2.6b to d) and their respective leaves (Fig. 2.6f) in Fig. 2.6 Table 2 presents the NSC vision model contrast values (△S) we obtained for each cultivar. We calculated △S values with leaves (L) and petals (P) to test floral contrast with leaf background. A floral pattern (e.g. bull's eye pattern) was tested by comparing the outer floral part (petal, P) with the central floral part (anthers, s). We also tested sepals as they are visible when petals are damaged or a cultivar has sparse inflorescence.

2.5.3 Leaves

Fig 2.6f demonstrates the minor variation in upper leaf reflectance across Fragaria sp. and cultivars indicating that the main factor in differing floral contrast and visibility to pollinators is solely the factor of floral pigments.

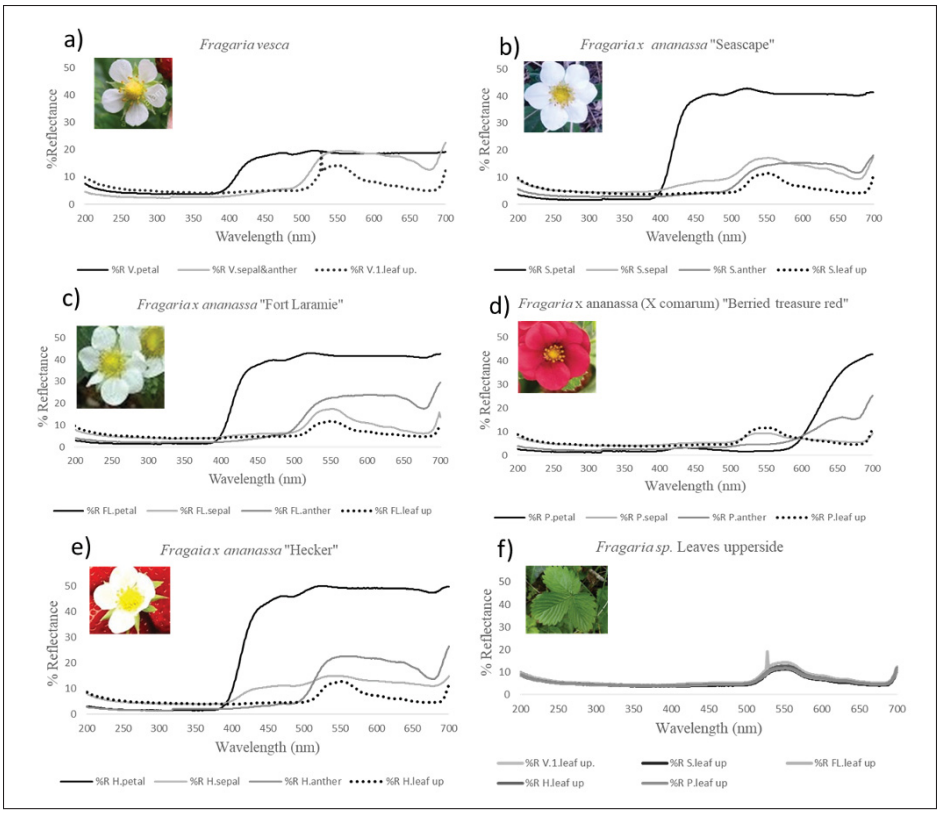

Figure 2.6 Reflectance spectrograms of Strawberry cultivars

2.5.4 Fragaria vesca

Fragaria vesca is a wild native strawberry species that has well-documented pollinator-flower interaction (Blažytė-Čereškienė, L. et al. 2012). Its spectrogram is published on the Floral Reflectance Database (FReD) and was used as a control for variation between studies. Our spectral reflectance curve showed the same pattern as previous reports (ref). The flower shows a distinct flower petal peak in the Bee blue range (spectral peak 424nm, Skorupski, P., & Chittka, L. 2010) and a sepal/anther peak in the Bee green range (spectral peak 539nm, Skorupski, P., & Chittka, L. 2010). A study by Martinez-Harms, J. et al. (2010) found that bees could detect flowers 75% of the time with a contrast value (△S) as low as 2.3. The contrast value for petal (△S=8.861) and sepal/anther (△S= 5.261) support the observations made in previous behavioural studies that this flower is visible to pollinators.

2.5.5 Fragaria x ananassa (x comarium) 'Berried treasure Red'

The red flowering cultivar, Fragaria x ananassa (x comarium) 'Berried treasure Red' (Fig.2.6 d), had floral peaks beyond 600nm and showed no contrast values between floral parts $\triangle S > 1.34$, indicating that bee pollinators would be blind to this cultivar. This cultivar, in particular, was bred purely for aesthetic appeal, with little regard for yield potential. It is not cultivated in fields and is a newer release to the consumer market.

2.5.6 White-flowering cultivars

When compared to their wild counterpart (Fig 2.6a), the white flowering cultivars "Seascape," "Fort Laramie," and "Hecker" (Fig 7, b, c, and e, respectively) exhibit higher petal reflectance, creating higher contrast and visibility for pollinators. These cultivars demonstrate petal peaks in the bee blue and anther peaks in bee Green (Spectral peak 539 nm, Skorupski, P., & Chittka, L. 2010). Anther/ petal contrast values indicate a discernable Bull's eye pattern for all three cultivars in the bee blue/ bee green range ($\triangle S$= 24.638, 24.651, and 28.027, respectively). The highest contrast value for all three cultivars was between petals and background leaves ($\triangle S$= 27.463, 27.127, and 33.086, respectively). "Hecker" had the highest contrast value with an L/P $\sim S$ = 33.086; 26.8% higher than its wild counterpart. "Hecker" is noted for producing large berries with good flavour (Bringhurst, R., & Voth, V., 1980). We know that insect pollination has a direct, positive effect on fruit quality (e.g., Nye, W. P., & Anderson, J. L.,1974; Wietzke, A., et al. 2018; Abrol, D. P., et al. 2019). In selectively breeding for higher yield and better-quality fruit, breeders could have inadvertently selected more visible flowers. As such, "Hecker" flowers would be more visible from the air to nearby pollinators than their conspecifics. Bees preferentially visit more visible targets when nectar rewards are equal (Spaethe, J. et al. 2001). The higher visitation rate by natural pollinators would positively affect the outcome of yield assessments.

2.5.7 Strawberry flowers in the UV

Gyan, K. Y. & Woodell, S. R. J. (1987) documented the spectrogram of the blackberry, Rubus fructicosus, which indicated a ~ 35% reflectance around 360nm. Almond cultivars, Prunus dulcis, have also shown a consistent, distinct peak at 350nm (Chen, B., Jin, Y., & Brown, P.,2019). Although the Fragaria genus shares the same family as Rubus, Fig. 7 does not indicate any reflectance peaks around 350-360 nm (or Bee UV, spectral peak 347nm, Skorupski, P., & Chittka, L. 2010) across all study species. Incidentally, there is minimal spectral reflectance in the near UV range (300-400nm). However, all the above samples exhibit an increase in reflection below 250nm. In this way, the Rosacea family shows reflection diversity in the near UV spectrum, indicating that findings from remote sensing or pollinator vision studies should not extend beyond the species or cultivar at hand.

Table 2.2 Visibility of Fragaria sp. floral parts to trichromatic insect pollinators. *Indicates above bee contrast detection threshold.

Cultivar	Floral parts contrasted	General trichromatic pollinator _S
Fragaria x ananassa (x comarium) 'Berried treasure Red'	A/S	1.165
	A/P	0.255
	S/P	1.309
	L/P	1.335
Fragaria vesca	A+S/P	*5.261
	L/P	*8.861
Fragaria x ananassa 'Hecker'	A/S	0.616
	A/P	*28.027
	S/P	*28.53
	L/P	*33.086
Fragaria x ananassa 'Fort Laramie'	A/S	*3.663
	A/P	*21.001
	S/P	*24.651
	L/P	*27.127
Fragaria x ananassa 'Seascape'	A/S	2.204
	A/P	*24.638
	S/P	*22.441
	L/P	*27.463

2.6 Conclusion

At this time, future floral reflectance studies should put more emphasis on crop species than native species. Our results showed a need for lightweight camera models for in-situ UV remote sensing. Current models are costly and cumbersome for automated deployment. The representation of crop families in the literature reflects their economic value in the global market. That being said,

UV reflectance is still a tiny proportion of all crop spectral reflectance studies. In analyzing the data we collected from Strawberry cultivars, we noted that commercial white-flowering strawberries produced a bull's eye contrast pattern in the bee-blue/ bee-green, producing the highest contrast with background leaves. The most notable, "Hecker," is prized for its production volume and high fruit quality. This may be due to its greater visibility to pollinators, i.e. bees, leading to higher pollination rates. Further studies presenting the spectral reflectance of crops across pollinator vision range (near UV to blue) would benefit pollinator interaction research and the agricultural industry and be an excellent resource for crop breeders.

2.7 Acknowledgements

We would like to that NSERC for funding this study. Our deepest thanks to Marie-Hélène Forget and the biology department at Laval University, Qc. for hosting us on their campus and for the loan of their lab equipment. Without both, this study would not have been possible.

Bibliography

Abrol, D. P., Gorka, A. K., Ansari, M. J., Al-Ghamdi, A. & Al-Kahtani, S. (2019). Impact of insect pollinators on yield and fruit quality of strawberry. *Saudi journal of biological sciences*, 26(3), 524-530.

Al-Mallahi, A., Kataoka, T., Okamoto, H. & Shibata, Y. (2010). Detection of potato tubers using an ultraviolet imaging-based machine vision system. *Biosystems engineering*, 105(2), 257-265.

Arnold, S., Savolainen, V. & Chittka, L. (2008). FReD: the floral reflectance spectra database. *Nature Precedings*, 1-1.

Balcerowska, G., Siuda, R., Skrzypczak, J., Łukanowski, A. & Sadowski, C. (2009). Effect of particle size and spectral sub-range within the UV-VIS-NIR range using diffuse reflectance spectra on multivariate models in evaluating the severity of fusariosis in ground wheat. *Food Additives and Contaminants*, 26(5), 726-732.

Bian, L., Cai, X. M., Luo, Z. X., Li, Z. Q. & Chen, Z. M. (2020). Foliage intensity is an important cue of habitat location for Empoasca onukii. *Insects*, 11(7), 426.

Blažytė-Čereškienė, L., Būda, V. & Bagdonaitė, E. (2012). Three wild Lithuanian strawberry species and their pollinators. *Plant systematics and evolution*, 298, 819-826.

Bringhurst, R. & Voth, V. (1980). Six new strawberry varieties released [California]. *California Agriculture California Agricultural Experiment Station*.

Briscoe, A. D. & Chittka, L. (2001). The evolution of color vision in insects. *Annual review of entomology*, 46(1), 471-510.

Brock, M. T., Lucas, L. K., Anderson, N. A., Rubin, M. J., Cody Markelz, R., Covington, M. F., Devisetty, U. K., Chapple, C., Maloof, J. N. & Weinig, C. (2016). Genetic architecture, biochemical underpinnings and ecological impact of floral UV patterning. *Molecular ecology*, 25(5), 1122-1140.

Brugger, A., Behmann, J., Paulus, S., Luigs, H.-G., Kuska, M. T., Schramowski, P., Kersting, K., Steiner, U. & Mahlein, A.-K. (2019). Extending hyperspectral imaging for plant phenotyping to the UV-range. *Remote Sensing*, 11(12), 1401.

Brugger, A., Schramowski, P., Paulus, S., Steiner, U., Kersting, K. & Mahlein, A. (2021). Spectral signatures in the UV range can be combined with secondary plant metabolites by deep learning to characterize barley–powdery mildew interaction. *Plant Pathology*, 70(7), 1572-1582.

Ceuppens, B., Ameye, M., Van Langenhove, H., Roldan-Ruiz, I. & Smagghe, G. (2015). Characterization of volatiles in strawberry varieties 'Elsanta'and 'Sonata'and their effect on bumblebee flower visiting. *Arthropod-Plant Interactions*, 9, 281-287.

Chen, B., Jin, Y. & Brown, P. (2019). An enhanced bloom index for quantifying floral phenology using multi-scale remote sensing observations. *ISPRS Journal of Photogrammetry and Remote Sensing*, 156, 108-120.

Chittka, L., Shmida, A., Troje, N. & Menzel, R. (1994). Ultraviolet as a component of flower reflections, and the colour perception of Hymenoptera. *Vision research*, 34(11), 1489-1508.

Cui, D., Li, M. & Zhang, Q. (2009). Development of an optical sensor for crop leaf chlorophyll content detection. *Computers and Electronics in Agriculture*, 69(2), 171-176.

Darwin, C. (1877). *The effects of cross and self fertilisation in the vegetable kingdom*. Ams PressInc.

Debnath, S., Paul, M., Rahaman, D. M., Debnath, T., Zheng, L., Baby, T., Schmidtke, L. M. & Rogiers, S. Y. (2021). Identifying individual nutrient deficiencies of grapevine leaves using hyperspectral imaging. *Remote Sensing*, 13(16), 3317.

Dias, P. A., Tabb, A. & Medeiros, H. (2018). Multispecies fruit flower detection using a refined semantic segmentation network. *IEEE robotics and automation letters*, 3(4), 3003-3010.

Eeraerts, M., Vanderhaegen, R., Smagghe, G. & Meeus, I. (2020). Pollination efficiency and foraging behaviour of honey bees and non-Apis bees to sweet cherry. *Agricultural and Forest Entomology*, 22(1), 75-82.

Feldhake, C. (2002). Beneficial spectral characteristics of red and black raspberry plants (Rubus idaeus and Rubus occidentalis). *Journal of Sustainable Agriculture*, 19(3), 65-76.

Folta, K. M. & Gardiner, S. E. (2009). *Genetics and genomics of Rosaceae*. Springer.

França-Silva, F., Rego, C. H. Q., Gomes-Junior, F. G., Moraes, M. H. D. d., Medeiros, A. D. d. & Silva, C. B. d. (2020). Detection of Drechslera avenae (Eidam) Sharif [Helminthosporium avenae (Eidam)] in black oat seeds (Avena strigosa Schreb) using multispectral imaging. *Sensors*, 20(12), 3343.

Guerra-Sanz, J. M. (2008). Crop pollination in greenhouses. *Bee pollination in agricultural ecosystems*, 27-47.

Gyan, K. Y. & Woodell, S. (1987). Analysis of insect pollen loads and pollination efficiency of some common insect visitors of four species of woody Rosaceae. *Functional Ecology*, 269-274.

Hansen, C., Steinmetz, H. & Block, J. (2021). How to conduct a meta-analysis in eight steps: a practical guide. *Springer*, 1-19.

HeadwallPhotonics. (2022). UV-vis 250-500nm [web page]. Retrieved from: https://www.headwallphotonics.com/products/uv-vis-250-500nm.

Henz, A., Debener, T. & Linde, M. (2015). Identification of major stable QTLs for flower color in roses. *Molecular breeding*, 35, 1-12.

Hirvonen, T., Orava, J., Penttinen, N., Luostarinen, K., Hauta-Kasari, M., Sorjonen, M. & Peiponen, K.-E. (2014). Spectral image database for observing the quality of Nordic sawn timbers. *Wood science and technology*, 48, 995-1003.

Ildiz, G. O., Celik, O., Atak, C., Yilmaz, A., Kabuk, H. N., Kaygisiz, E., Ayan, A., Meric, S. & Fausto, R. (2020). Raman Spectroscopic and Chemometric Investigation of Lipid–Protein Ratio Contents of Soybean Mutants. *Applied Spectroscopy*, 74(1), 34-41.

International Light Technologies, I. (2019). What is The Difference Between a Spectrometer, a Spectroradiometer, and a Radiometer? [web page]. Retrieved from: https://www.intl-lighttech.com/blog/what-difference-between-spectrometer-spectroradiometer-and-radiometer.

Jan, S., Kamili, A. N., Parray, J. A., Bedi, Y. S. & Ahmad, P. (2016). Microclimatic variation in UV perception and related disparity in tropane and quinolizidine alkaloid composition of Atropa acuminata, Lupinus polyphyllus and Hyoscyamus niger. *Journal of Photochemistry and Photobiology B: Biology*, 161, 230-235.

Jones, C., Jones, J. & Lee, W. (2010). Diagnosis of bacterial spot of tomato using spectral signatures. *Computers and Electronics in Agriculture*, 74(2), 329-335.

Klatt, B. K., Holzschuh, A., Westphal, C., Clough, Y., Smit, I., Pawelzik, E. & Tscharntke, T. (2014). Bee pollination improves crop quality, shelf life and commercial value. *Proceedings of the Royal Society B: Biological Sciences*, 281(1775), 20132440.

Klem, K., Ač, A., Holub, P., Kováč, D., Špunda, V., Robson, T. M. & Urban, O. (2012). Interactive effects of PAR and UV radiation on the physiology, morphology and leaf optical properties of two barley varieties. *Environmental and experimental botany*, 75, 52-64.

Koger, C. H., Shaw, D. R., Reddy, K. N. & Bruce, L. M. (2004a). Detection of pitted morningglory (Ipomoea lacunosa) with hyperspectral remote sensing. II. Effects of vegetation ground cover and reflectance properties. *Weed Science*, 52(2), 230-235.

Koger, C. H., Shaw, D. R., Reddy, K. N. & Bruce, L. M. (2004b). Detection of pitted morningglory (Ipomoea lacunosa) by hyperspectral remote sensing. I. Effects of tillage and cover crop residue. *Weed science*, 52(2), 222-229.

Koski, M. H. & Ashman, T. (2014). Dissecting pollinator responses to a ubiquitous ultraviolet floral pattern in the wild. *Functional Ecology*, 28(4), 868-877.

Kovar, M., Brestic, M., Sytar, O., Barek, V., Hauptvogel, P. & Zivcak, M. (2019). Evaluation of hyperspectral reflectance parameters to assess the leaf water content in soybean. *Water*, 11(3), 443.

Lee, W., Hodgkinson, I. & Johnson, P. (1990). A test for ultraviolet reflectance from fleshy fruits of New Zealand plant species. *New Zealand journal of botany*, 28(1), 21-24.

Li, X., Chen, Y. & Bond, T. C. (2016). Light absorption of organic aerosol from pyrolysis of corn stalk. *Atmospheric Environment*, 144, 249-256.

Liu, H., Lee, S.-H. & Chahl, J. S. (2017). A multispectral 3-D vision system for invertebrate detection on crops. *IEEE Sensors Journal*, 17(22), 7502-7515.

Liu, H., Lee, S.-H. & Chahl, J. S. (2018). Registration of multispectral 3D points for plant inspection. *Precision Agriculture*, 19, 513-536.

Liu, Y., Cheng, T., Zhu, Y., Tian, Y., Cao, W., Yao, X. & Wang, N. *Conference Proceedings n°issue number. Comparative analysis of vegetation indices, non-parametric and physical retrieval methods for monitoring nitrogen in wheat using UAV-based multispectral imagery*. 2016 IEEE International Geoscience and Remote Sensing Symposium (IGARSS). IEEE.

Malacara, D. *Conference Proceedings n°issue number*. Color vision and colorimetry: theory and applications. Spie Bellingham, WA.

Mangelsdorf, A. J. & East, E. (1927). Studies on the genetics of Fragaria. *Genetics*, 12(4), 307.

Martínez-Harms, J., Palacios, A., Márquez, N., Estay, P., Arroyo, M. T. & Mpodozis, J. (2010). Can red flowers be conspicuous to bees? Bombus dahlbomii and South American temperate forest flowers as a case in point. *Journal of Experimental Biology*, 213(4), 564-571.

Merzlyak, M. N., Solovchenko, A. E., Smagin, A. I. & Gitelson, A. A. (2005). Apple flavonols during fruit adaptation to solar radiation: spectral features and technique for non-destructive assessment. *Journal of plant physiology*, 162(2), 151-160.

Mirza, A. U., Kareem, A., Nami, S. A., Bhat, S. A., Mohammad, A. & Nishat, N. (2019). Malus pumila and Juglen regia plant species mediated zinc oxide nanoparticles: synthesis, spectral characterization, antioxidant and antibacterial studies. *Microbial pathogenesis*, 129, 233-241.

Morandin, L., Laverty, T. & Kevan, P. (2001). Bumble bee (Hymenoptera: Apidae) activity and pollination levels in commercial tomato greenhouses. *Journal of economic entomology*, 94(2), 462-467.

Morandin, L. A., Laverty, T. M., Gegear, R. J. & Kevan, P. G. (2002). Effect of greenhouse polyethelene covering on activity level and photo-response of bumble bees. *The Canadian Entomologist*, 134(4), 539-549.

Moyers, B. T., Owens, G. L., Baute, G. J. & Rieseberg, L. H. (2017). The genetic architecture of UV floral patterning in sunflower. *Annals of botany*, 120(1), 39-50.

Muchhala, N., Johnsen, S. & Smith, S. D. (2014). Competition for hummingbird pollination shapes flower color variation in Andean Solanaceae. *Evolution*, 68(8), 2275-2286.

Ngo, V.-D., Kang, S.-W., Ryu, D.-K., Chung, S.-O., Park, S.-U., Kim, S.-J. & Park, J.-T. (2013). Location and number of sampling for optical reflectance measurement of Chinese cabbage and kale leaves. *IFAC Proceedings Volumes*, 46(18), 241-246.

Nye, W. P. & Anderson, J. L. (1974). Insect Pollinators Frequenting Strawberry Blossoms and the Effect of Honey Bees on Yield and Fruit Quality1. *Journal of the American Society for Horticultural Science*, 99(1), 40-44.

Papiorek, S., Junker, R. R., Alves-dos-Santos, I., Melo, G. A., Amaral-Neto, L. P., Sazima, M., Wolowski, M., Freitas, L. & Lunau, K. (2016). Bees, birds and yellow flowers: pollinator-dependent convergent evolution of UV patterns. *Plant Biology*, 18(1), 46-55.

Patel, K. K., Kar, A. & Khan, M. (2019). Potential of reflected UV imaging technique for detection of defects on the surface area of mango. *Journal of food science and technology*, 56, 1295-1301.

Peters, R. D. & Noble, S. D. (2014). Spectrographic measurement of plant pigments from 300 to 800 nm. *Remote sensing of environment*, 148, 119-123.

Prasad, B., Carver, B. F., Stone, M. L., Babar, M., Raun, W. R. & Klatt, A. R. (2007). Potential use of spectral reflectance indices as a selection tool for grain yield in winter wheat under great plains conditions. *Crop science*, 47(4), 1426-1440.

PrecedenceResearch. (2022). Commercial greenhouse merket [web page]. Retrieved from: https://www.precedenceresearch.com/commercial-greenhouse-market.

Qi, Y., Bai, S. & Heisler, G. M. (2003). Changes in ultraviolet-B and visible optical properties and absorbing pigment concentrations in pecan leaves during a growing season. *Agricultural and Forest Meteorology*, 120(1-4), 229-240.

Ray, S., Jain, N., Miglani, A., Singh, J., Singh, A., Panigrahy, S. & Parihar, J. (2010). Defining optimum spectral narrow bands and bandwidths for agricultural applications. *Current Science*, 1365-1369.

Rivera-Romero, C. A., Palacios-Hernández, E. R., Trejo-Durán, M., Rodríguez-Liñán, M. d. C., Olivera-Reyna, R. & Morales-Saldaña, J. A. (2020). Visible and near-infrared spectroscopy for detection of powdery mildew in Cucurbita pepo L. leaves. *Journal of Applied Remote Sensing*, 14(4), 044515-044515.

Rodríguez-Gironés, M. A. & Telles, F. J. (2020). The normalized segment classification model: A new tool to compare spectral reflectance curves. *Ecology and Evolution*, 10(24), 13872-13882.

Santoyo-Mora, M., Sancen-Plaza, A., Espinosa-Calderon, A., Barranco-Gutierrez, A. I. & Prado-Olivarez, J. (2019). Nondestructive quantification of the ripening process in banana (Musa AAB Simmonds) using multispectral imaging. *Journal of Sensors*, 2019.

Schroder, M. L., Kruger, K., Glinwood, R. & Ignell, R. (2014). Visual cues and host-plant preference of the bird cherry-oat aphid, Rhopalosiphum padi (Hemiptera: Aphididae). *African Entomology*, 22(2), 428-436.

Shahbandeh, M. (2023a). Global production of fresh fruit from 1990 to 2021 [web page]. Retrieved from: https://www.statista.com/statistics/262266/global-production-of-fresh-fruit/#:~:text=In%202021%2C%20the%20global%20production,million%20metric%20tons%20in%202000.

Shahbandeh, M. (2023b). Global production of vegetables in 2021 [web page]. Retrieved from: https://www.statista.com/statistics/264065/global-production-of-vegetables-by-type/.

Sharma, N., Khajuria, Y., Sharma, J., Tripathi, D. K., Chauhan, D. K., Singh, V. K., Kumar, V. & Singh, V. K. (2018). Microscopic, elemental and molecular spectroscopic investigations of root-knot nematode infested okra plant roots. *Vacuum*, 158, 126-135.

Shrestha, B. P., Guyer, D. E. & Ariana, D. P. *Conference Proceedings n°issue number. Opto-electronic determination of insect presence in fruit.* Monitoring Food Safety, Agriculture, and Plant Health. SPIE.

Siuda, R., Balcerowska, G. & Sadowski, C. (2006). Comparison of the usability of different spectral ranges within the near ultraviolet, visible and near infrared ranges (UV-VIS-NIR) region for the determination of the content of scab-damaged component in blended samples of ground wheat. *Food additives and contaminants*, 23(11), 1201-1207.

Skorupski, P. & Chittka, L. (2010). Photoreceptor spectral sensitivity in the bumblebee, Bombus impatiens (Hymenoptera: Apidae). *PLoS One*, 5(8), e12049.

Smeesters, L., Meulebroeck, W., Raeymaekers, S. & Thienpont, H. (2016). Non-destructive detection of mycotoxins in maize kernels using diffuse reflectance spectroscopy. *Food Control*, 70, 48-57.

Spaethe, J., Tautz, J. & Chittka, L. (2001). Visual constraints in foraging bumblebees: flower size and color affect search time and flight behavior. *Proceedings of the National Academy of Sciences*, 98(7), 3898-3903.

Spectrecology. (2021). Spectrometer vs. Spectrophotometer. [web page]. Retrieved from: https://spectrecology.com/blog/spectrometer-vs-spectrophotometer/#:~:text=Like%20mentioned%20previously%2C%20spectrometers%20measure, absorption%20spectrum%20of%20the%20samplea.

Takiguchi, Y., Nakayama, M., Kubota, M. & Yamazaki, J. (1998). New color TV cameras for ultraviolet, near infrared and visible light. *IEEE transactions on broadcasting*, 44(1), 123-130.

Thomasson, J. A. & Sui, R. (2009). Cotton leaf reflectance changes after removal from the plant. *Journal of Cotton Science*, 13(3), 206-211.

Utech, F. H. & Kawano, S. (1975). Spectral polymorphisms in angiosperm flowers determined by differential ultraviolet reflectance. *The botanical magazine= Shokubutsu-gaku-zasshi*, 88, 9-30.

Varliklioz Er, S., Eksi-Kocak, H., Yetim, H. & Boyaci, I. H. (2017). Novel spectroscopic method for determination and quantification of saffron adulteration. *Food analytical methods*, 10, 1547-1555.

Venturello, A., Ceccarelli, R., Garrone, E. & Geobaldo, F. (2012). FAST NON-DESTRUCTIVE DETERMINATION OF CHLOROPHYLLS IN APPLE SKIN. *Italian Journal of Food Science*, 24(2).

Wang, C.-Y., Tang, L., Jiang, T., Zhou, Q., Li, J., Wang, Y.-Z. & Kong, C.-H. (2021). Geographical traceability of Eucommia ulmoides leaves using attenuated total reflection Fourier transform infrared and ultraviolet-visible spectroscopy combined with chemometrics and data fusion. *Industrial Crops and Products*, 160, 113090.

Wang, X., Huang, J., Li, Y. & Wang, R. *Conference Proceedings n°issue number. Rice leaf area index (LAI) estimates from hyperspectral data.* Ecosystems Dynamics, Ecosystem-Society Interactions, and Remote Sensing Applications for Semi-Arid and Arid Land. SPIE.

Weng, S., Yu, S., Guo, B., Tang, P. & Liang, D. (2020). Non-destructive detection of strawberry quality using multi-features of hyperspectral imaging and multivariate methods. *Sensors*, 20(11), 3074.

Wietzke, A., Westphal, C., Gras, P., Kraft, M., Pfohl, K., Karlovsky, P., Pawelzik, E., Tscharntke, T. & Smit, I. (2018). Insect pollination as a key factor for strawberry physiology and marketable fruit quality. *Agriculture, ecosystems & environment*, 258, 197-204.

Wójtowicz, M., Wójtowicz, A. & Piekarczyk, J. (2016). Application of remote sensing methods in agriculture. *Communications in biometry and crop science*, 11(1), 31-50.

Xue, J. & Su, B. (2017). Significant remote sensing vegetation indices: A review of developments and applications. *Journal of sensors*, 2017.

Yang, C. & Lee, W. S. *Conference Proceedings n°issue number. Spectral signatures of blueberry fruits and leaves*. 2011 Louisville, Kentucky, August 7-10, 2011. American Society of Agricultural and Biological Engineers.

Yang, W., Li, M., Zheng, L. & Sun, H. *Conference Proceedings n°issue number. Prediction of nitrogen content of jujube leaves based on NIR spectra*. 2014 Montreal, Quebec Canada July 13–July 16, 2014. American Society of Agricultural and Biological Engineers.

Yang, X., Heisler, G. M., Montgomery, M. E., Sullivan, J. H., Whereat, E. B. & Miller, D. R. (1995). Radiative properties of hardwood leaves to ultraviolet irradiation. *International journal of biometeorology*, 38, 60-66.

Yoshioka, Y., Horisaki, A., Kobayashi, K., Syafaruddin, Niikura, S., Ninomiya, S. & Ohsawa, R. (2005). Intraspecific variation in the ultraviolet colour proportion of flowers in Brassica rapa L. *Plant breeding*, 124(6), 551-556.

Zhang, C. & Kovacs, J. M. (2012). The application of small unmanned aerial systems for precision agriculture: a review. *Precision agriculture*, 13, 693-712.

Zhang, M., Hale, A. & Luedeling, E. *Conference Proceedings n°issue number. Feasibility of using remote sensing techniques to detect spider mite damage in stone fruit orchards*. IGARSS 2008-2008 IEEE International Geoscience and Remote Sensing Symposium. IEEE.

Zhang, Y., Zheng, L., Li, M., Deng, X. & Ji, R. (2015). Predicting apple sugar content based on spectral characteristics of apple tree leaf in different phenological phases. *Computers and Electronics in Agriculture*, 112, 20-27.

CHAPTER 3

SEE AS A BEE: UV SENSOR FOR AERIAL STRAWBERRY CROP MONITORING

3.1 Contribution from other Authors

Corentin Boucher and Ryan Brown contributed to the 3D-printed attachment prototype and initial field deployment. Ali Imran produced the orthomosaic from the field validation footage for the final analysis and acted as a visual observer during field validation. David St-onge provided editorial notes and proofreading for the final journal submission.

Megan Heath[1] , Ali Imran [1] , David St-Onge[1]

[1] Département de Génie Mécanique, École de Technologie Supérieure, École de technologie supérieure, Montreal, Quebec, Canada
1100 Notre-Dame Ouest, Montréal, Québec, Canada H3C 1K3

Article submitted for review « environmental stream » in March 2023.

3.2 Abstract

Ultraviolet (UV)-reflectance is an essential signal of many plant species which use wavelength-selective pigments in floral reproductive structures to determine the colour of flowers and how they appear to their aerial pollinators, primarily bees. This paper presents a pollinator-inspired remote sensing system incorporating UV-reflectance into a flower detector for strawberry crops. We designed a compact, cost-effective UV-sensitive camera for aerial remote sensing over crop rows. Our camera and a deep-learning algorithm comprised our Nature Inspired Detector (NID)system. We trained YOLO V5 and Faster R-CNN on our dataset of strawberry images incorporating the UV spectrum (300-400nm). Our results showed that NID YOLO V5 outperformed NID Faster R-CNN in training time (0.3 vs. 4.5-5.5 hours) and mAP (0.951 vs. 0.934). We also present the field test of our NID YOLOv5 system on a drone platform to validate its ability to detect strawberry flowers.

3.3 RÉSUMÉ

La réflectance ultraviolette (UV) est un signal essentiel de nombreuses espèces végétales qui utilisent des pigments sélectifs en longueur d'onde dans les structures reproductives florales pour déterminer la couleur des fleurs et leur apparence pour leurs pollinisateurs aériens, principalement les abeilles. Cet article présente un système de télédétection inspiré des pollinisateurs incorporant la réflectance UV dans un détecteur de fleurs pour les cultures de fraises. Nous avons conçu une caméra sensible aux UV compacte et économique pour la télédétection aérienne sur les rangées de cultures. Notre caméra et un algorithme d'apprentissage en profondeur comprenaient notre

système de détecteur inspiré de la nature (NID). Nous avons formé YOLO V5 et Faster R-CNN sur notre ensemble de données d'images de fraises incorporant le spectre UV (300-400nm). Nos résultats ont montré que NID YOLO V5 surpassait NID Faster R-CNN en temps d'entraînement (0,3 contre 4,5-5,5 heures) et mAP (0,951 contre 0,934). Nous présentons également le test terrain de notre système NID YOLOv5 sur une plateforme drone pour valider sa capacité à détecter les fleurs de fraisier.

3.4 Introduction

Agriculture is known to be one of the most active sectors of innovation (Davis, J. et al., 2018). Now more than ever, with the changing dynamics of the world due to climate change, urbanization, and the increased human population, the agriculture sector needs to adapt and expand its adoption of automated systems for crop management. Several technologies can support the required innovations, namely compact digital cameras, supervised machine learning algorithms, and mobile robotic systems such as uncrewed aerial vehicles (UAVs). As the accessibility to these technologies increases, UAV remote sensing is quickly becoming the tool of choice across agricultural (Tsouros et al., 2019) and non-agricultural (Shakhatreh et al., 2019) sectors for data gathering. Various remote sensors enable the capture, processing, and analysis of airborne data to provide farmers with accurate information about their crops and help them make informed decisions (e.g., needs-based water application, nutrients, and chemicals). Such is the basis of precision agriculture. In parallel, the industry underwent significant development in robotized crop manipulation, such as harvesters and pollinators. The latter is motivated by the near-extinction of several species of bees in some parts of the world (e.g., Goulson, D. 2012). Indeed, according to Aurell et al. (2022), the honey bee population decreased by 23.8% in 2021-2022. Moreover, some modern agricultural practices, often beneficial to industry and society, provide an unsuitable environment for natural pollinators (bees), such as greenhouses and poly-tunnels (Kopongo, J.P. et al., 2008). Similarly, the growing popularity of urban agriculture and vertical farms calls for creative innovation for the sustainable pollination of crops (Goldstein, 2018). The development of digital cameras, using (charge-coupled device) CCD and

(complementary metal oxide semiconductor) CMOS sensors, more powerful computers, and object detection algorithms have been crucial to precision agriculture. Today, neural network algorithms combined with (Red, green, blue) RGB or hyperspectral camera data have given rise to vegetation indices that can measure soil and plant health, crop growth, and nutrient requirements (Kattenborn et al., 2021). It also shows excellent potential for weed and disease detection, input requirements, and crop yield estimation (Tsouros et al., 2019). Yield can be estimated based on flower count or stand count. Manual flower counts are labour-intensive and prone to human error (Chen Y. et al., 2019). A robotic system must first detect and localize the target flowers to automate counting. Unlike the detection and localization of ripe fruits (Chen Y. et al., 2019), flower detection can direct robotic pollination efforts rather than robotic picking. Knowing flower time and location also helps farmers predict harvest time and inform fertilization and watering schedules. UAV-mounted cameras and artificial intelligence (AI) software allow automated, non-subjective yield estimation at a fraction of the cost and effort. Most existing remote sensing systems are modelled on human vision (RGB), mimicking farmers observing their fields. However, flowering plants have co-evolved for millennia to interact with insects whose vision spans the UV-G-B range (Briscoe & Chittka, 2001). Pollinating insects such as honey bees (Apis sp.) can distinguish crop species and cultivars from one another based on floral patterning undetectable to human vision (Briscoe & Chittka, 2001) against a complex background and while airborne. These pollinators' increased contrast in the UV-G-B spectrum contributes significantly to their target detection time. We hypothesize that the UV-G-B range would be better suited to UAV platforms for flower detection as it would mimic pollinator vision and detect intended plant cues for aerial pollinators. This paper presents a biologically inspired UV-G-B camera, Nature Inspired Detector (NID), which mimics a natural pollinator's vision for detecting crop flowers using state-of-the-art object detection algorithms tuned to the task. We will start by introducing the most relevant works regarding agricultural remote sensing platforms and sensors. A related works subsection discussing detection algorithms will appear later in the learning to see flowers section. We then present our study species, sensor design, and detection algorithm. We conclude with our field deployment of the NID system.

3.4.1 Related work

3.4.1.1 Aerial remote sensing platforms

Several options for ground vehicles are already available as remote sensing and phenotyping platforms (Deery et al., 2014; Williams et al., 2020). As for artificial pollinators, uncrewed ground vehicle (UGV)-based robotic systems have already been proposed for Kiwi fruit pollination (Li et al., 2022; Williams et al., 2020) and used in poly-tunnels (Ko et al., 2014; Le et al., 2020). Nevertheless, recent years have seen a tendency toward using UAVs for precision agriculture (Kim et al., 2019; Mulla, 2013). Various aerial platforms are available: their selection depends on the application requirements. Fixed-wing platforms have increased flight time and payload capacity; however, their inability to hover makes it challenging to get higher-quality data. Blimps can obtain clear images due to their hovering ability but are slow and challenging to maneuver outdoors. Rotor copters also have hovering capabilities, thus providing a better chance to capture higher-quality imagery. However, these platforms have limited flight times (Sankaran et al., 2015). Sankaran et al. (2015) present a comprehensive review of the advantages and disadvantages of different types of platforms for applications in agriculture. In this project, we selected a quadcopter as our platform because of the ability to control the flight speed and altitude to collect high-quality images embedded with GPS location data for map creation. Although the speed and fight time is less than that of a fixed-wing, this project is testing the NID sensor. Therefore, we chose the platform which would collect the highest quality data.

3.4.1.2 Visual remote sensing and detection

The most frequently used optoelectronic sensors for precision agriculture applications use the visible light range (>400nm; Pallottino F. et al., 2019). When capturing images, these lightweight, inexpensive sensors replicate roughly the human vision range (400-700nm). They benefit from the most extensive literature on object detection algorithms due to the many RGB image datasets available for classification (Deng J. et al., 2009). Detecting flowers and fruits using these sensors has led to different algorithms, such as flower contour detection through

colour and edge detection (Hong & Choi, 2001) and spectral and spatial methods, e.g., for detecting tomatoes (Senthilnath et al., 2016). However, their main disadvantage is the inability to analyze any parameter outside the visual spectrum (Tsouros et al., 2019). Other spectral bands offer valuable data about the crops, such as the state of chlorophyll. Naturally, when a plant becomes diseased or stressed, the amount of chlorophyll reduces - resulting in an overall change in spectral reflectance. Studies have also shown that UAV-based NIR imagery can accurately detect water stress (Antolinez et al., 2022; Z. Zhou et al., 2021). As such, multispectral cameras, visual sensors that detect in more than one spectral range, are growing in popularity in agriculture. For example, Abdulridha et al. (2020) showed that a robotic system including a Vis-NIR multispectral camera (400-950nm) could detect powdery mildew in asymptomatic squash plants with 89% accuracy under field conditions. Gomez-Candon et al. (2016) used a similar sensor to study water stress in apple orchards. They showed a strong correlation (R^2 = 0,9975) between temperature measured on ground targets and estimates made from aerial images. Alternatively, Stumph et al. (2019) used a UV-VIS multispectral camera to detect tree-dwelling insects using induced fluorescence and achieved detection precision as high as 80%. Thus, there is much potential for remote detection beyond the visual range (400-700nm) of RGB cameras. The Near UV (300-400nm) is one underexplored range in multispectral cameras. Although we present the example of Stumph et al. (2019) above, their study measured UV fluorescence rather than UV reflectance. As previously discussed, flowering plants have co-evolved interactions with insects using UV reflectance in the Near UV range (Briscoe & Chittka, 2001). Remote sensing data of this type would capture ecological signalling and further the understating of pollinator landscapes.

3.4.1.3 UV Cameras

UV cameras are expensive and cumbersome (Stuart et al., 2019). The lack of development of such sensors may come from the need for studies exploring the use of UV floral reflectance of plants. Spectral reflectance studies have reported down to 300nm, but most species in reflectance databases are native species, not crops (Arnold et al., 2008). The lack of data on the floral

reflectance of crops leaves a knowledge gap for estimating the visibility of crop cultivars to pollinators. Furthermore, UV cameras and lenses in plant UV spectral reflectance studies were bulky and expensive, leading to even fewer field studies (Stuart et al., 2019). This project aims to develop an efficient, biologically inspired flower detection system that leverages the UV-G-B spectrum using a powerful yet cost-effective drone setup.

3.4.1.4 Strawberry as the target species

Rosacea is one of the major flowering crops families cultivated globally. It contains orchard species (e.g., apple, pear) as well as bramble (e.g., Raspberries, Blackberries) and alpine berry species (e.g., strawberry, cloudberry). Unlike Rosacea orchard and bramble crops, some commercial strawberry cultivars are everbearing, flowering throughout the growing season. Their prolific flowering, compact habit, and flowers held on stocks above the foliage make it an ideal crop for aerial imagery studies. Strawberry fruit is Canada's fifth most valuable fruiting crop and is an ever-growing market, increasing consistently since 2015, peaking in 2021 and earning a farm gate value of $129 million. With the post-pandemic consumer market prioritizing local and domestic food production (Beingessner, N. et al. 2020), provinces are incorporating more greenhouse production to make local produce available year-round, leading sales of greenhouse strawberries to increase by 19.1% in 2021 (Statistics Canada, 2022; Government of Canada, 2022; Government of Saskatchewan, 2023). Quebec is the country's leading producer and has more fields devoted to strawberry production than any other province (Statistical Overview of the Canadian Fruit Industry 2021, 2022; Fig. 1). However, with a recent commitment to reducing the use of pesticides and unpredictable weather, overall production per hectare has declined, leading Quebec also to consider greenhouse and polytunnel strawberry production. As previously mentioned, greenhouse environments can be challenging to natural pollinators. With greenhouse production and domestic fruit consumption only predicted to increase, robotic pollinators are a technology on the horizon for Canadian fruit farmers.

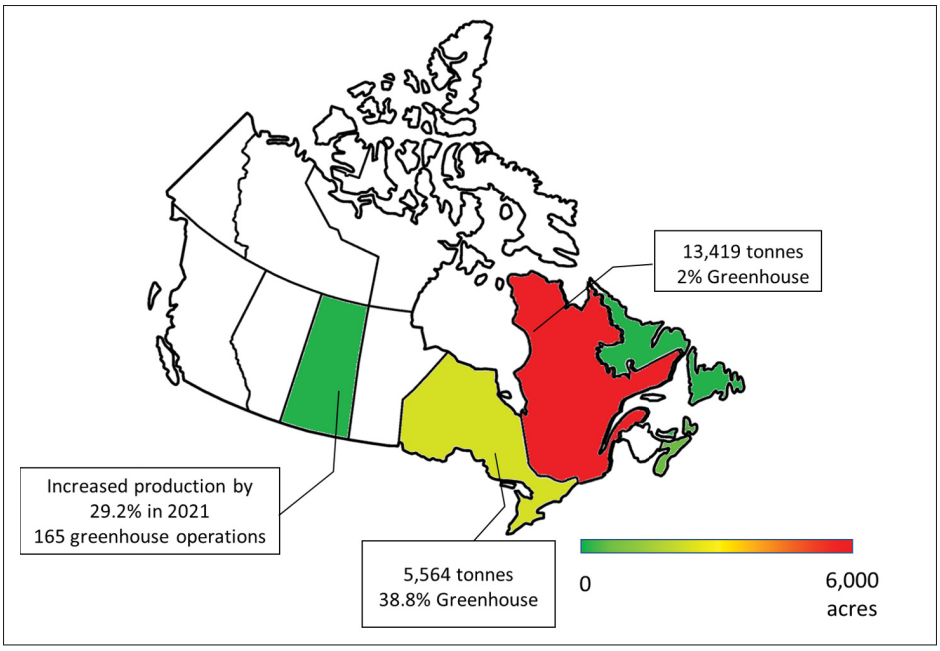

Figure 3.1 2021 Canadian farm distribution map for strawberry fruit production (Statistics Canada, 2022; Government of Canada, 2022; Government of Saskatchewan, 2023).

3.5 Sensor Design

We postulated that UV-based detection would enhance airborne flower count, but adapted remote sensors were missing. So, we designed a custom sensor inspired by bees. In agricultural settings, various bee species are the primary pollinators of strawberry flowers, primarily Apis mellifera, or western honey bees (James & Pitts-Singer, 2008). Like humans, bees have three peaks in their vision spectrum. While humans see from 400-700nm, from blue to red (RGB), honey bees see from 300-650nm, from near-UV to green (Briscoe & Chittka, 2001). Fig. 2 presents the respective sensitivity curves. The design of most digital cameras captures images in the human visual spectrum using a Bayer filter, a pattern of red, green, and blue filters (RGB) across the photodiode matrix (Palum, 2001). The internal body of most cameras also has an Anti-Aliasing (AA) (blur)/ IR cut filter (ICF) made of various glass, which prevents UV light from reaching the sensor due to the absorption of photon energy (Ulizio, 2015). Internal microlens and external glass lenses also affect UV light transmission similarly. Figure 4(a) shows the internal spectral

transmission of an industry-standard GoPro camera. For our Nature inspired detector (NID)to capture images in the near UV-B-G range we first removed the Bayer filter from a CMOS sensor to facilitate this. Lopez-Ruiz et al. (2017) accomplished this with their UV sensor for a Raspberry Pi camera; however, the process needed to be more robust and replicable. Therefore, we partnered with a commercial company to remove the filter for us using their proprietary methodology (MaxMax, 2022). We replaced the AA/ICF with Schott WG280 glass which transmits light to 280nm (Schott AG, 2023). We removed the micro lens, and added an external lens to restrict the transmission above 650 nm, which allowed 80-100This design results in a monochrome sensor that mimics the vision spectrum of a western honey bee. Inherently, monochrome sensors can achieve higher resolution, faster processing times or frame rates, and store smaller files than their RGB counterparts, as coloured images are processed over three dimensions. The Bayer filter can also reduce the optical resolution of the system (Burlayenko, O. V., & Lukianchuk, O. V., 2017). In this context, monochrome images present several advantages for machine vision processing. Figure 4 contrasts a standard GoPro's internal light transmission design to our NID camera.

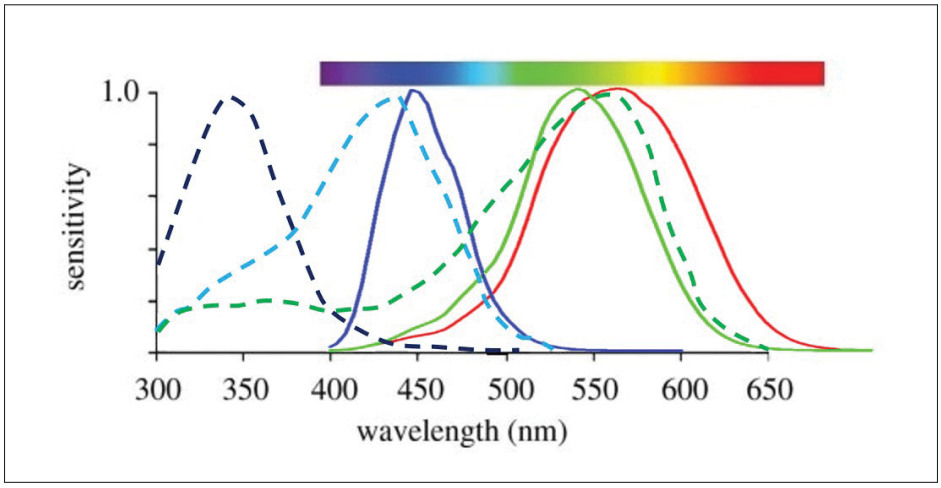

Figure 3.2 Visual spectral Sensitivity of Western Honey Bee v.s. Human. Dotted black, blue, and green lines represent bee UV, B, G. Solid red, green and blue lines represent human R, G, and B (Coliban et al., 2020; Dyer et al., 2015).

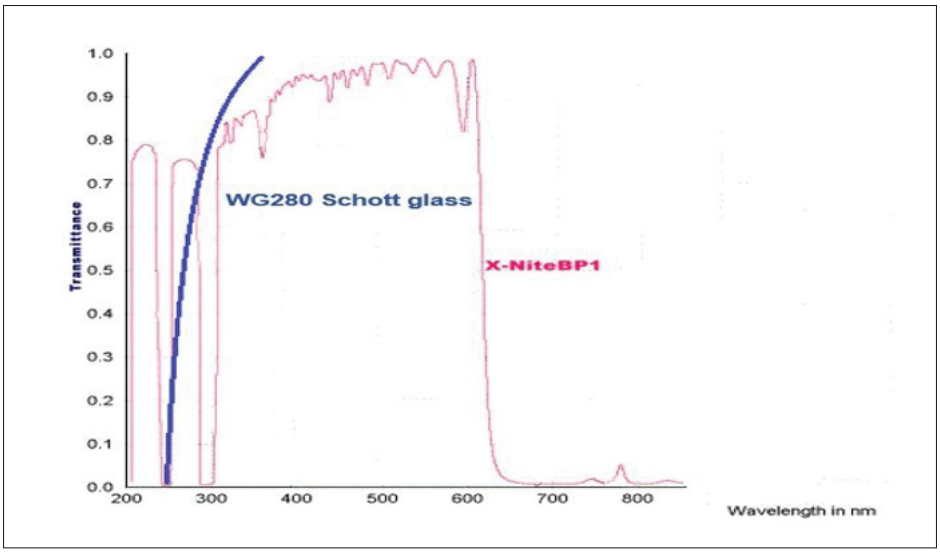

Figure 3.3 Transmission spectrograph for materials of NID camera. The blue line represents WG280 Schott glass, and the pink line represents the XNite BP1 filter. >80 % transmission in the 300-650nm range (LDP LLC - MAXMAX, 2022; Schott AG., 2023).

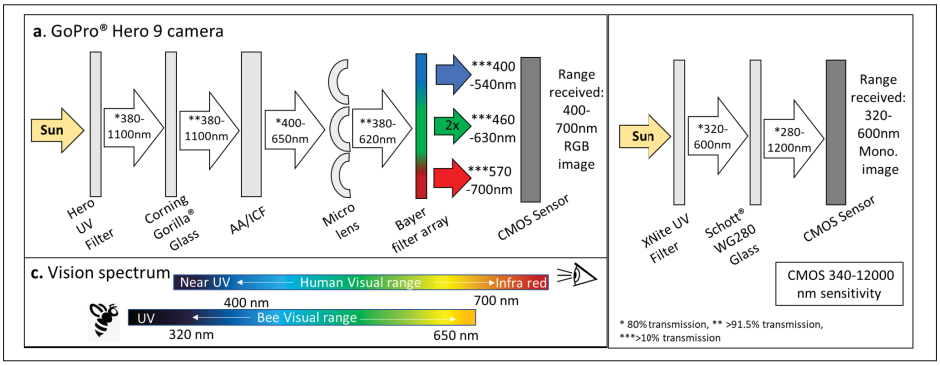

Figure 3.4 Internal visual remote sensor design. (a) GoPro Hero 9 RGB action camera (b) NID monochrome camera. * 80% transmission, ** >91.5% transmission, ***>10% transmission. (Bandara A.M.R.R, 2011; Taguchi, H., & Enokido, M., 2017; Nieto, D., et al. 2012; Präzisions Glas & Optik., 2023; Dyer et al., 2015; Corning Inc., 2022)

3.5.1 Camera Design

We designed the body of our NID to be lightweight, affordable, and drone-mountable. Given the shipping conditions for the 2019 pandemic, Table 1 compares two camera body models we considered. Both are lightweight and can mount onto a drone. When considering camera resolution requirements, we considered that the downdraft from rotors could move target flowers and introduce excess blur to images, decreasing data quality. To keep downdraft effects to a minimum, we designed the system to fly at 3m. When determining the appropriate sensor resolution, we sampled comparable flower detection studies which used ground sampling distance (GSD) as a standard metric across various camera remote sensors, which ranged from 0.7 to 3 cm/pixel (Chen et al., 2019; Hunt Jr & Daughtry, 2018; Vanbrabant et al., 2020). For digital photos in remote sensing, GSD is a geometric relationship, described in equation 1, between a camera's physical attributes and distance from a target to determine ground measurements from pixel distances in an image (Purcell, C. R. 2000). Considering our pre-determined flight altitude of 3m, we determined that a resolution of 3264x2448 would result in a GSD= 1.16cm/pixel. Both models considered had sensors that could provide an adequate resolution. However, unlike the GoPro, the X-Nite has a USB cable connecting the camera directly to a computer for image capture and continuous power drawing. This camera is lighter weight and retails for 500 USD. These attributes made it more robust and cost-effective than the GoPro model.

Table 3.1 Test of a long table caption, with Our camera model contrasted with a comparable camera on the market

Camera	Body Weight (g)	Lens Weight (g)	Body Dim. (LxWxH) cm	Cable (15cm) Weight (g)	Total
X-Nite	83	4	4x 2.2 x 4	7	87-91g
GoPro HERO 9	158	na	5.5 x 7.1 x 3.3	na	158g

We calculated GSD with the following:

$$GSD = \lambda * H/c \tag{3.1}$$

where H is the flight altitude (m), c, the Focal length (mm), and λ, the camera sensor pixel size.

3.5.2 Camera Characterization

Characterization of a camera model has applications in developing and using colour-related image-processing algorithms (Barnard, K., & Funt, B. 2002). It ensures a predictive relationship between the camera sensor's response as a function of wavelength. Previous studies have quantitatively analyzed the colour patterns of animals in the UV spectrum using linear camera responses (Garcia JE et al., 2013). As the NID is a novel design, we characterized the camera to ensure a linear response for analyzing strawberry flowers similarly. A reflectance standard is a reference sample of a known reflectance ratio (amount of light reflected by a surface given a determined amount of incident radiation) within a given spectral range (Wen, BJ. 2016). As commercially available reflectance standards poorly reflect UV (320-400 nm), we created appropriate reflectance standards. Following the work of Dyer et al. (2004), we created five standards from varying proportions of medical-grade magnesium oxide (MgO), Plaster of Paris, and activated carbon and a sixth standard of black UV-absorbing plastic. We measured each standard's (1-6) spectral reflectance (% R) in the 200 - 700 nm range with a Perkin Elmer's Lambda 850 UV-VIS spectrophotometer. Figure 6 shows the resulting spectrogram. The intercept for each curve denotes the consistent % R each standard will emit across varying lighting conditions. Images of the standards were recorded with our NID camera in raw monochrome format and encoded into an 8-bit scale using ImageJ (1.53t). The camera response consisted of mean pixel values obtained from point sampling ten pixels at the center region of each standard. Calculations involved in characterization were performed in Microsoft® Excel® 2016. The Opto-electronic conversion function curve for the NID was constructed by plotting the camera's response for each spectral reflectance reading (%R) of the reflectance standards (Garcia JE et al., 2014). A simple linear model was fitted to the curve, providing strong evidence

for a linear relationship between the camera response, pixel value, and spectral reflectance (Fig 5. R2 = 0.9821).

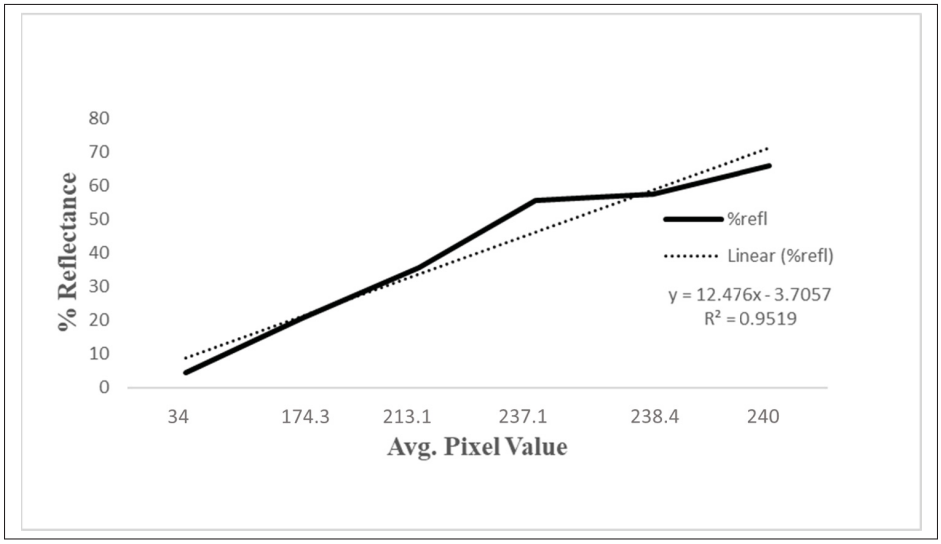

Figure 3.5 Correlation curve for UV-reflectance standards and image pixel values. % Reflectance measured with Perkin Elmer's Lambda 850 UV-VIS spectrophotometer. Pixel value from images produced with the NID camera.

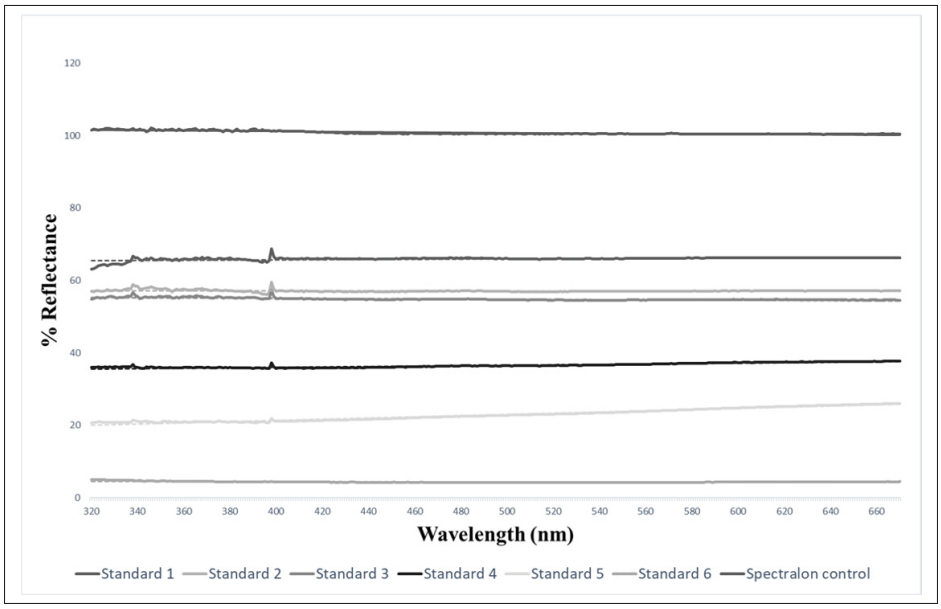

Figure 3.6 UV reflectance standards spectrogram measured with Perkin Elmer's Lambda 850 UV-VIS spectrophotometer.

3.6 Learning to see flowers

Whereas detection algorithms on RGB images have gone a long way, multispectral images are only recently being used (e.g., Zeng Z et al., 2021). Using our NID camera design, we developed a detection algorithm adapted and trained on its specific type of images. Pre-trained algorithms, such as MSCOCO, only use RGB image datasets. It was, therefore, necessary to create a training dataset of unique images for our target species and sensor. Validation determines which algorithm is best for flower detection in this context. In competition, Convolutional Neural Networks (CNN) have proven themselves to be the best approach for target identification and classification due to their ability to extract increasingly complex visual features through their hierarchical structure (Zheng et al., 2021). Regarding strawberry flower counting, Faster Region-based Convolutional Neural Networks (RCNN) have shown the best results (86.1%, 86.4%, and 86% accuracy, respectively (Chen et al., 2019; Lin & Chen, 2018 and Zhou et al., 2020). In an aerial application, Chen et al. (2019) recently employed Faster R-CNN for strawberry flower detection with a DJI Phantom 4 pro and attained mAP= 0.772. Given their flight altitude of 3m and a mixed training data set of strawberry cultivars, this is the most recent comparable work to our current study. However, Faster RCNN often has a longer processing time than You Only Look Once (YOLO) object detection (Mahendrakar et al., 2022). Furthermore, Immaneni et al. tested YOLOV4 drone images from a strawberry field and achieved a better accuracy; of 91.95% at 14.6 FPS (Immaneni et al., 2022; Bochkovskiy et al., 2020). Related species, such as Pear flowers, have also shown promising results with YOLO, with an mAP of 94% (Wang et al., 2022).

3.6.1 Captured Strawberry flower dataset

Since no image datasets of UV-B-G images were available, we created an original dataset using various strawberry cultivars and made it publicly available in PytorchYoloV5 and TF record formats (DOI: 10.5281/zenodo.7863719). F. x ananassa ‘Seascape’ and ‘Fort Laramie’ are commonly recommended commercial everbearing cultivars for central and east coast Canadian provinces. Therefore, we included them along with F. x ananassa ‘Hecker,’ an older everbearing

cultivar popular with commercial growers for decades before ‘Seascape’(Strawberry Plants LLC, 2022). F. Vesca is a North American woodland native grown by breeders for its genetic attributes and by specialty fruit growers for wine production. We procured and potted all bare-root plants from a local Quebec nursery. We captured images under sunny conditions between 11 am and 1 pm within the 320-600nm. We placed the camera 6cm from an open flower at a 90-degree overhead angle. Images had 640x480 resolution (focal length= 3.6mm, GSD=0.023 cm/pixel). We used Roboflow Inc. (2022) for data management and bounding box image labelling. Images were pre-processed for auto-orientation and resized into a square shape of 416x416 for detection algorithm compatibility. We then applied the following augmentations of the dataset: horizontal and vertical flip, rotate ±90-degrees, rotate ±15-degrees, sheer ±15-degrees vertical and horizontal, noise 5%, and blur 5px. The resulting dataset consisted of 284 NID images (Table 3.2).

3.7 Algorithm comparison

We tested two CNN architectures on our dataset for flower detection: Faster R-CNN and YOLO V5. We chose Faster R-CNN to compare our results to the work of Chen et al. (2019), who detected strawberry flowers from RGB UAV images, currently the closest related work to our study. Where they used Resnet 50 as their convolutional layer architecture, we chose Incecption V2, which produces a higher detection accuracy (Bianco S. et al., 2018; Sukegawa S. et al., 2022). We included YOLO architecture, a classic one-stage object detection algorithm for real-time detection. The fifth generation, YOLO V5, was employed following a recent review by Tian, M., & Liao, Z. (2021) analysing the algorithm’s performance for flower detection. We based our code implementation on the publicly available script for both YoloV5 (Jocher et al., 2020) and Faster R-CNN (Ren et al., 2015). Initially, we used pre-trained weights for both algorithms from MS COCO2017 (Lin et al., 2014). Training, validation, and test split was 40%/40%/20%. We compared the algorithms using the following metrics: mAP@0.5, True positive (TP), False positive (FP), and False negative (FN). mAP value allows for algorithm comparison in the machine learning discipline, whereas TP is most relevant in practical agriculture. We trained

YOLO and Faster R-CNN on our data set to compare results. YOLOV5s was chosen due to its better performance on the small custom training datasets (e.g. Ouf, N. S., 2023) and ran for 1000 epochs with 16 batches. We ran Faster R-CNN with inception V2 for 20000 steps with 12 batches. Both algorithms used early stopping during training to prevent overfitting. Table 3 shows the results for the trained algorithms. YOLOV5s showed overall higher performance than Faster R-CNN. Therefore, we used YOLOv5s for field testing of the system.

Table 3.2 Hyperparameters of detection algorithms

HYPERPARAMETER	Yolo V5	Faster R-CNN
Momentum	0.937	0.9
Intersection over threshold	0.2	0.934
Epochs	1000	20000
Image size	640x480	640x480
Data Augmentation	horizontal and vertical flip, rotate ±90-degrees, rotate ±15-degrees, sheer ±15-degrees vertical and horizontal, noise 5%, and blur 5px	horizontal and vertical flip, rotate ±90-degrees, rotate ±15-degrees, sheer ±15-degrees vertical and horizontal, noise 5%, and blur 5px
Batch size	16	12

Table 3.3 Resulting detection from UVGB trained YOLOV5 and Faster R-CNN on training dataset at 416x416 resolution, and, on aerial images at 96x96 resolution

Training Dataset	Detection Method	mAP @0.5	Detection count	FP(Rate)	TP(Rate)	FN(Rate)
96x96	YOLOv5	0.951	3260	2042 (62.2%)	1218 (37.1%)	25 (0.76%)
96x96	FR-CNN V2	0.934	166	108(8.0%)	58(4.3%)	1185 (87.7%)
416x416	YOLOv5	0.978	77	0 (0%)	77 (97.4%)	2 (2.53%)
416x416	FR-CNN V2	0.912	144	69 (46.31%)	75 (50.34%)	5 (3.36%)

3.8 Field deployment

To validate the usefulness of our solution as a precision agriculture tool, we deployed our sensor on a commercial UAV and flew over a local strawberry field.

3.8.1 Aerial System implementation

We selected the UAV platform to maximize the payload capacity while minimizing cost and size. Table 4 details the comparison of the potential options we considered. Spiri Mu (2023) stood out as the best option compared to other commercially available devices. The Mu is powered by Nvidia's TX2, powerful enough for heavy onboard image processing. To mount our camera and interface it to the onboard computer, we replaced the original underbelly of the Mu with an in-lab 3D printed attachment which could house the mounting for the camera. Moreover, we replaced the original landing gear of the drone with wooden dowels to make it taller to accommodate the additional sensor. Figure 8 shows the modified drone in the field, ready for take-off. Qground Control (QGC) calibrates onboard sensors and monitors mission parameters during flight. The onboard system runs on Linux with ROS preinstalled, simplifying our sensors' software integration and providing us with tools to record and transmit data efficiently. Our ROS camera driver is based on standard ROS packages to fetch and convert the USB camera feed to a ROS image topic. Figure 7 shows an excerpt of the training data set.

3.8.2 Field deployment setup

We conducted field flights at Pépinère F. Fortier near Princeville, Qc. -planted with a mix of white-flowering 'Seascape' and 'Albion' cultivars. An altitude of 3m reduced the effects of rotor downdraft on plants and produced a GSD=1.16cm/ pixel. The Mu captured video under sunny conditions from 11 am-1 pm to keep consistent with the training dataset. We used 88 frames, which were tiled and re-sized to 768x768 pixels to reduce processing time, to test our trained algorithm. A single reviewer counted 2295 flowers as the ground truth.

Figure 3.7 Strawberry cultivars. * RGB images from Vesey, 2022, ** monochrome images captured with NID camera. The far-right image shows Yolo's detection of a strawberry flower on the training dataset.

3.8.3 Flower detection on UAV images

The flower resolution from aerial images was much lower than the training dataset. We, therefore, trained YoloV5 and Faster R-CNN on the same image dataset as before but at a lower resolution, 96x96 pixels, to increase TP detection (Table 3). We ran inferences with a 0.51 confidence threshold on a Tesla P100-PCIE - 16 GB in Google Colab (Bisong, 2019). Tables 5 shows the results of our trained YOLOV5 on the aerial images.

Table 3.4 Cost and size comparison of similar UAV models on the market with the Spiri Mu

Drone	Dimensions LxWxH (mm)	Payload Capacity (g)	Base Cost (CAD)
Spiri Mu	170x170x51	1000	2000
DJI M300	810×670×430	2700	12,722
DJI Mavic 3	347.5×283×107.7	727.4	2544
DJI Phantom 4	289.5x289.5x196	800	2383

3.9 Results

3.9.1 Flower detection from aerial images

Although the TP detection proportion was low (37.1 percent) for YoloV5, overall, 97 percent of flowers were accurately detected (n=1218 of 1243 in the dataset). However, the FP detections (n=2042,62.2 percent) far outnumbered the TP leading to a lower proportion. Ripening or developing fruits accounted for 33.3% (n=680) of FP detections 8b.

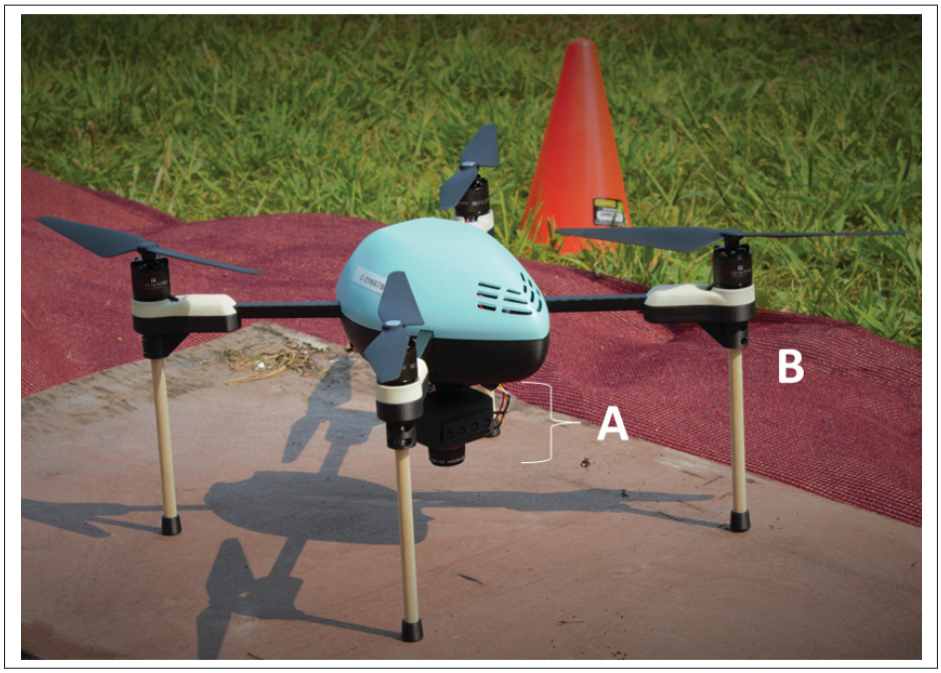

Figure 3.8 Modified Spiri Mu quadcopter. (A) NID camera held on the underside of UAV facing the ground at 90 degrees. (B) Extended legs to accommodate NID camera mounting.

A similar result was attained with Faster R-CNN (17.6 %). YOLO V5 showed the overall best performance for our system. As we did not train our algorithm with strawberry fruits, and they exhibited similar spectral properties as the flowers, this led to increased FP detections (see, for instance, Fig. 9).

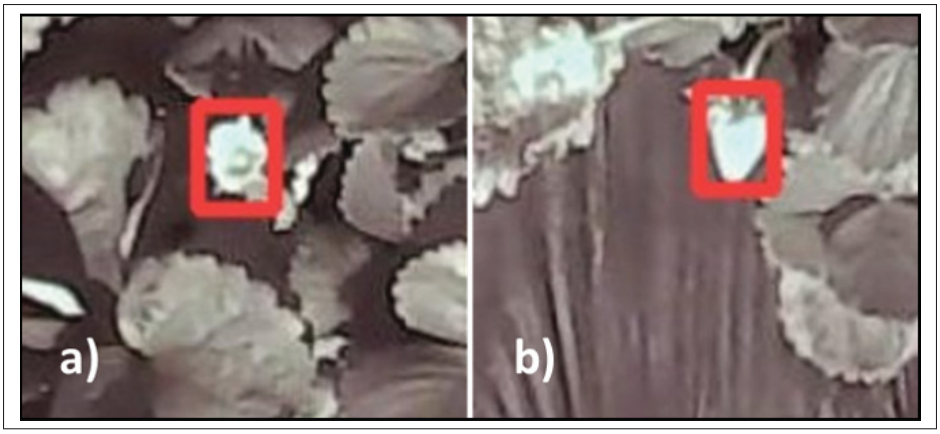

Figure 3.9 Detection examples from aerial images of (a) TP detections of open flowers and (b) FP from ripening fruits.

Chen et al. (2019) conducted a similar flower detection study on strawberries using a Phantom 4 Pro to capture aerial images in RGB. Table 5 compares their results with ours. Chen et al. (2019) used Faster R-CNN with Resnet50 trained on Imagenet at a flight altitude of 3m. Our system used Inception V2, resulting in higher mAP with Faster R-CNN than their study; however, overall detection was low. When comparing the results from the NID to the findings from Chen et al. (2019), the NID showed a higher detection accuracy (mAP) with a higher image processing time (FPS). This result can be attributed to the difference in CNN architecture as Inception V2 does produce higher accuracy but is much slower than Resnet50 (Bianco S. et al., 2018; Sukegawa S. et al., 2021). Our YoloV5 algorithm vastly outperformed Faster R-CNN algorithms in training time (0.3 vs. 4.5-5.5 hours), mAP (mAp=0.951 vs mAP= 0.934-0.772) and image processing (14.5 vs. 0.54 or 8.872 FPS) and was therefore used in our field validation.

3.9.2 Orthomosaic of field

We Orthomosaiced 742 video frames using Pix4D software (Pix4D SD, 2023) with 80% overlap, synchronized with GPS coordinates (Fig. 10a).

We isolated one row comprising 57 frames (Fig. 10 b & c) and manually counted 33 flowers for ground truth—Table 6 and Figure 10 d & e present the results of the NID system on the

Table 3.5 Comparison of sensors in similar experimental conditions. NID detection results on aerial images using YoloV5 and Faster R-CNN compared with Faster R-CNN from Chen et al. (2019).

UAV Model	Detection Method	Training Time (Hrs)	mAP@0.5	FPS
Spiri Mu	YOLOv5	0.3	0.951	0.0083
Spiri Mu	FR-CNN Inc.V2	4.5	0.934	1.86
Phantom 4 Pro	FR-CNN with Resnet50	5.5	0.772	8.872

orthomosaic. Overall, 90.9% of flowers were accurately detected (n=30 of 33 in the row). Patterns of FP, TP and FN rates are consistent with NID detection on individual video frames. However, the higher FP rate could be attributed to stitching effects from the orthomosaic. Ripening or developing fruits accounted for 28.6% (n=45) of FP detections which is also consistent with results from individual aerial frames.

Table 3.6 Orthomosaic. Algorithm detection vs. ground truth.

Training dataset resolution	Detection Method	mAP@0.5	Detection count	FP rate	TP rate	FN rate
94*94	YOLOv5	0.951	190	157(81.3%)	30(15.5%)	3(1.55%)

3.10 Discussion

Farmers, like the ones from our test field, re-plant yearly for the best harvest results. A tool for flower detection would need to be robust to changing varieties and cultivars and provide consistent results. Farmers had randomly planted the test field with 'Seascape' and 'Albion' cultivars. Although we included 'Seascape' in our initial training dataset, 'Albion' was not. Our algorithm detected novel cultivar flowers, indicating that a limited database of strawberry

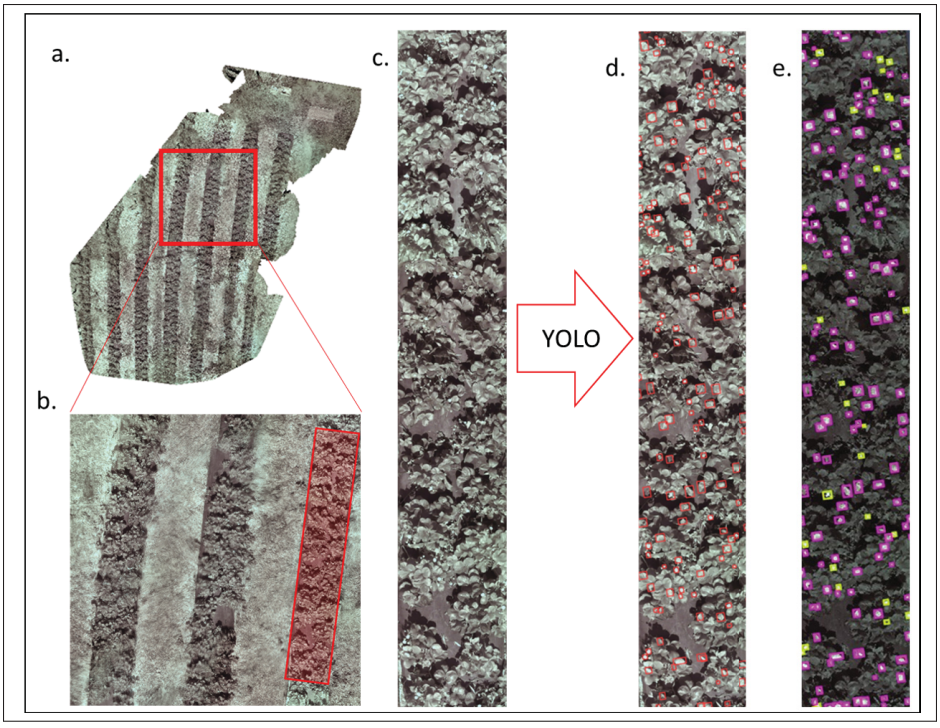

Figure 3.10 Orthomosaic image analysis. (a) orthomosaic image of Quebec strawberry farm from NID field deployment. (b) isolated crop row in the field. (c) isolated crop row (d) Detected flowers with YOLOv5 NID (e) Labelled detections from YOLOv5 NID system; Yellow for flowers, pink for False positives.

cultivar flowers could be sufficient for developing remote sensing tools and would only require finite updating to accommodate new varieties to the market. Schaefer, et al. (2008) explored the effects of fruit colour variation as signals of dietary reward. They found that fruits rich in anthocyanins, a plant antioxidant, are black or UV- reflecting and are in higher concentrations in ripe fruits. In strawberry fruits, anthocyanin concentration increases with fruit maturity (da Silva, et al.,2007; Song et al. 2015). As our camera perceives the UV but not Red spectral range, ripening strawberries appear bright white in our frames. When at similar size and circularity, these fruits are mislabelled as flowers by our algorithm (Fig 9). The remaining FP detections can be attributed to solar reflection on leaves, runners, and flower stocks. These are examples of the complexity of our field setting. Including null images of background foliage in initial training would also increase overall algorithm robustness. However, no FP was attributed to

weed species visible within and between crop rows. These included: Fleabane, lambs' quarter, crabgrass, purslane, and cow vetch. Some of these plants were in flower; however, the algorithm could distinguish between these and strawberry blossoms. We consider this worthy of future exploration. A significant limitation of this research was the aerial resolution of the flowers. Due to the downdraft effects from the rotors, we could not reduce flight altitude beyond 3m. This leads us to reduce the initial training image resolution significantly to match the drone images. A higher resolution sensor would help detection while maintaining flight altitude and avoiding downdraft effects.

3.11 Conclusion

In this paper, we have described and discussed the development of a cost-effective, lightweight, airborne UV-sensitive camera. We performed extensive field experimentation to gather high-quality imagery data and demonstrated its usability by feeding it to two state-of-the-art object detection algorithms. The improved results over previous similar experiments show that our system is highly scalable, as the cost of the system is low, and that the UV spectrum can provide valuable information about the crops' flowers. The development of this sensor and the choice of the aerial platform opens up opportunities for future work. Developing a flower detector is the first step towards the bigger goals, such as estimating crop yields and creating a functional, biologically inspired robotic pollinator. Currently, using ROS onboard of Spiri Mu drone, GPS coordinates and ROS topics are recorded. In the future, these GPS coordinates can be used in conjunction with the images to create a global field map and direct harvest efforts. Additionally, developing automatic row cropping methodologies would help get better results with the object detection algorithms. Future iterations of this study will also include strawberry fruits at various developmental stages in the initial training process. Our sensor design shows a linear relationship between percent reflectance and pixel value between 300 and 650 nm opening up many possibilities for its use even beyond agriculture. Our design can be ordered to specification, and the sensor transmission spectra are provided upon request. Lastly, our monochrome sensor design does not allow for the contrast between chroma channels as RGB

sensors or animal eyes do. Future sensor iterations should explore removing only the red colour of the Bayer filter. Using our existing camera body design, this would retain the green and blue channels and replace the red with UV. We could perform computer analysis for 3-channel images routinely, as the proportion and placement of the three channels on the sensor diode are unchanged. Thus, several enhancements to this platform can improve the overall performance of the system and can help us make significant contributions to accelerate the research in this area. We openly make our datasets and trained algorithms available in hopes of furthering scientific pursuits.

3.12 Acknowledgments

We must thank Spiri Robotics for lending us a platform to conduct our field deployment. Corentin Boucher and Ryan Brown were also essential to the success of prototype adaptation and field deployment. We also thank Pr. Marcel Babin and his team at Takuvik in the University of Laval, Canada, for lending us their spectrophotometer to characterize our sensor.

3.13 Disclosure statement

No conflict of interest was reported by the author (s).

3.14 Funding

NSERC funded this research through the UTILI CREATE program.

3.15 ORCID

Authors ORCID number: 0000-0002-0587-8598

Bibliography

Abdulridha, J., Ampatzidis, Y., Roberts, P. & Kakarla, S. C. (2020). Detecting powdery mildew disease in squash at different stages using UAV-based hyperspectral imaging and artificial intelligence. *Biosystems engineering*, 197, 135-148.

Antolínez García, A. & Cáceres Campana, J. W. (2022). Identification of pathogens in corn using near-infrared UAV imagery and deep learning. *Precision Agriculture*, 1-24.

Arnold, S., Savolainen, V. & Chittka, L. (2008). FReD: the floral reflectance spectra database. *Nature Precedings*, 1-1.

Bandara, A. (2011). *A music keyboard with gesture controlled effects based on computer vision*. (Thesis).

Barnard, K. & Funt, B. (2002). Camera characterization for color research. *Color Research & Application: Endorsed by Inter-Society Color Council, The Colour Group (Great Britain), Canadian Society for Color, Color Science Association of Japan, Dutch Society for the Study of Color, The Swedish Colour Centre Foundation, Colour Society of Australia, Centre Français de la Couleur*, 27(3), 152-163.

Beingessner, N. & Fletcher, A. J. (2020). "Going local": Farmers' perspectives on local food systems in rural Canada. *Agriculture and Human Values*, 37, 129-145.

Bisong, E. (2019). *Building machine learning and deep learning models on Google cloud platform*. Springer.

Bochkovskiy, A., Wang, C.-Y. & Liao, H.-Y. M. (2020). Yolov4: Optimal speed and accuracy of object detection. *arXiv preprint arXiv:2004.10934*.

Burlayenko, O. V. & Lukianchuk, O. V. *Conference Proceedings n° issue number. Increasing of optical resolution of photos*. 2017 IEEE International Young Scientists Forum on Applied Physics and Engineering (YSF). IEEE.

Canada, S. (2022a). Strawberry fields forever? [web page]. Retrieved from: https://www150.statcan.gc.ca/n1/daily-quotidien/220426/dq220426e-eng.htm.

Canada, S. (2022b). Strawberry fields forever? [web page]. Retrieved from: https://www.statcan.gc.ca/o1/en/plus/1300-strawberry-fields-forever.

Chen, Y., Lee, W. S., Gan, H., Peres, N., Fraisse, C., Zhang, Y. & He, Y. (2019). Strawberry yield prediction based on a deep neural network using high-resolution aerial orthoimages. *Remote Sensing*, 11(13), 1584.

Coliban, R.-M., Marincaş, M., Hatfaludi, C. & Ivanovici, M. (2020). Linear and non-linear models for remotely-sensed hyperspectral image visualization. *Remote Sensing*, 12(15), 2479.

da Silva, F. L., Escribano-Bailón, M. T., Alonso, J. J. P., Rivas-Gonzalo, J. C. & Santos-Buelga, C. (2007). Anthocyanin pigments in strawberry. *LWT-Food Science and Technology*, 40(2), 374-382.

Davis, J. (2018). 5 innovative industries that are growing fast. Market Research Blog [web page]. Retrieved from: https://blog.marketresearch.com/5-innovative-industries-that-are-growing-fast.

Deery, D., Jimenez-Berni, J., Jones, H., Sirault, X. & Furbank, R. (2014). Proximal remote sensing buggies and potential applications for field-based phenotyping. *Agronomy*, 4(3), 349-379.

Deng, J., Dong, W., Socher, R., Li, L.-J., Li, K. & Fei-Fei, L. *Conference Proceedings n°issue number*. *Imagenet: A large-scale hierarchical image database*. 2009 IEEE conference on computer vision and pattern recognition. Ieee.

DJI. (2023a). Dji Mavic 3 specs [web page]. Retrieved from: https://www.dji.com/ca/mavic-3/specs.

DJI. (2023b). Dji phantom 4 pro [web page]. Retrieved from: https://www.dji.com/ca/phantom-4-pro/info.

Dyer, A. G., Garcia, J. E., Shrestha, M. & Lunau, K. (2015). Seeing in colour: a hundred years of studies on bee vision since the work of the Nobel laureate Karl von Frisch. *Proceedings of the Royal Society of Victoria*, 127(1), 66-72.

Dyer, A. G., Muir, L. & Muntz, W. (2004). A calibrated gray scale for forensic ultraviolet photography. *Journal of forensic sciences*, 49(5), 1056-1058.

Garcia, J. E., Rohr, D. & Dyer, A. G. (2013). Trade-off between camouflage and sexual dimorphism revealed by UV digital imaging: the case of Australian Mallee dragons (Ctenophorus fordi). *Journal of Experimental Biology*, 216(22), 4290-4298.

Garcia, J. E., Wilksch, P. A., Spring, G., Philp, P. & Dyer, A. (2014). Characterization of digital cameras for reflected ultraviolet photography; implications for qualitative and quantitative image analysis during forensic examination. *Journal of forensic sciences*, 59(1), 117-122.

Goldstein, H. (2018). The green promise of vertical farms [Blueprints for a Miracle]. *IEEE Spectrum*, 55(6), 50-55.

GoPro. (2023). Hero 9 Black Manual [web page]. Retrieved from: https://gopro.com/content/dam/help/hero9-black/manuals/HERO9Black_UM_ENG_REVB.pdf.

Goulson, D. (2012). Decline of bees forces China's apple farmers to pollinate by hand. *China Dialogue*, 2, 2012.

Gómez-Candón, D., Virlet, N., Labbé, S., Jolivot, A. & Regnard, J.-L. (2016). Field phenotyping of water stress at tree scale by UAV-sensed imagery: new insights for thermal acquisition and calibration. *Precision agriculture*, 17, 786-800.

Hong, S.-W. & Choi, L. *Conference Proceedings n°issue number*. *Automatic recognition of flowers through color and edge based contour detection*. 2012 3rd International conference on image processing theory, tools and applications (IPTA). IEEE.

Hunt Jr, E. R. & Daughtry, C. S. (2018). What good are unmanned aircraft systems for agricultural remote sensing and precision agriculture? *International journal of remote sensing*, 39(15-16), 5345-5376.

Immaneni, A. & Chang, Y. K. *Conference Proceedings n°issue number*. *Real-time counting of strawberry using cost-effective embedded GPU and YOLOv4-tiny*. 2022 ASABE Annual International Meeting. American Society of Agricultural and Biological Engineers.

Inc., C. (2022a).). Corning® Gorilla® Glass Victus® 2. Corning Gorilla® Glass [web page]. Retrieved from: https://www.corning.com/microsites/csm/gorillaglass/PI_Sheets/Gorilla_Glass_Victus_2_PI_Sheet.pdf.

Inc., R. (2022b). Explore the Roboflow Universe. The world's largest collection of open source computer vision datasets and APIs [web page]. Retrieved from: https://universe.roboflow.com/.

James, R., James, R. R. & Pitts-Singer, T. L. (2008). *Bee pollination in agricultural ecosystems*. Oxford University Press on Demand.

Jocher, G., Stoken, A., Borovec, J., Changyu, L. & Hogan, A. (2020). ultralytics/yolov5: v3. 1-bug fixes and performance improvements. *Zenodo*.

Kapongo, J. P., Shipp, L., Kevan, P. & Broadbent, B. (2008). Optimal concentration of Beauveria bassiana vectored by bumble bees in relation to pest and bee mortality in greenhouse tomato and sweet pepper. *BioControl*, 53, 797-812.

Kattenborn, T., Leitloff, J., Schiefer, F. & Hinz, S. (2021). Review on Convolutional Neural Networks (CNN) in vegetation remote sensing. *ISPRS journal of photogrammetry and remote sensing*, 173, 24-49.

Kesteloo, H. (2020). Dji matrice 300 specifications and zenmuse h20 hybrid thermal camera [web page]. Retrieved from: https://dronedj.com/2020/01/21/dji-matrice-300-specifications-zenmuse-h20-hybrid-camera/.

Kim, J., Kim, S., Ju, C. & Son, H. I. (2019). Unmanned aerial vehicles in agriculture: A review of perspective of platform, control, and applications. *Ieee Access*, 7, 105100-105115.

Ko, M. H., Ryuh, B.-S., Kim, K. C., Suprem, A. & Mahalik, N. P. (2014). Autonomous greenhouse mobile robot driving strategies from system integration perspective: Review and application. *IEEE/ASME Transactions On Mechatronics*, 20(4), 1705-1716.

Le, T. D., Ponnambalam, V. R., Gjevestad, J. G. & From, P. J. (2020). A low-cost and efficient autonomous row-following robot for food production in polytunnels. *Journal of Field Robotics*, 37(2), 309-321.

Li, K., Zhai, L., Pan, H., Shi, Y., Ding, X. & Cui, Y. (2022). Identification of the operating position and orientation of a robotic kiwifruit pollinator. *Biosystems Engineering*, 222, 29-44.

Lin, P. & Chen, Y. *Conference Proceedings n°issue number. Detection of strawberry flowers in outdoor field by deep neural network*. 2018 IEEE 3rd International Conference on Image, Vision and Computing (ICIVC). IEEE.

Lin, T.-Y., Maire, M., Belongie, S., Hays, J., Perona, P., Ramanan, D., Dollár, P. & Zitnick, C. L. *Conference Proceedings n°issue number. Microsoft coco: Common objects in context*. Computer Vision–ECCV 2014: 13th European Conference, Zurich, Switzerland, September 6-12, 2014, Proceedings, Part V 13. Springer.

LLC, S. R. (2023). Spiri Mu [web page]. Retrieved from: https://spirirobotics.com/products/spiri-mu/.

Lopez-Ruiz, N., Granados-Ortega, F., Carvajal, M. A. & Martinez-Olmos, A. (2017). Portable multispectral imaging system based on Raspberry Pi. *Sensor Review*.

Luo, M. R. (2016). *Encyclopedia of color science and technology*. Springer New York.

Mahendrakar, T., Ekblad, A., Fischer, N., White, R., Wilde, M., Kish, B. & Silver, I. *Conference Proceedings n°issue number*. *Performance Study of YOLOv5 and Faster R-CNN for Autonomous Navigation around Non-Cooperative Targets*. 2022 IEEE Aerospace Conference (AERO). IEEE.

MAXMAX, L. L. (2022a). IR Filters [web page]. Retrieved from: https://www.maxmax.com/filters.

MAXMAX, L. L. (2022b). Maxmax monochrome camera module [web page]. Retrieved from: https://maxmax.com/shopper/product/15991-xniteusb8m-m-usb-2-0-8megapixel-monchrome-camera-mod.

Mulla, D. J. (2013). Twenty five years of remote sensing in precision agriculture: Key advances and remaining knowledge gaps. *Biosystems engineering*, 114(4), 358-371.

Nieto, D., Vara, G., Diez, J. A., O'Connor, G. M., Arines, J., Gómez-Reino, C. & Flores-Arias, M. T. (2012). Laser-based microstructuring of surfaces using low-cost microlens arrays. *Journal of Micro/Nanolithography, MEMS, and MOEMS*, 11(2), 023014-023014.

of Canada, G. (2022). Statistical overview of the Canadian fruit industry 2021 [web page]. Retrieved from: https://agriculture.canada.ca/en/sector/horticulture/reports/statistical-overview-canadian-fruit-industry-2021#a1.4.

of Saskatchewan, G. (2023). Greenhouses. Government of Saskatchewan [web page]. Retrieved from: https://www.saskatchewan.ca/business/agriculture-natural-resources-and-industry/agribusiness-farmers-and-ranchers/crops-and-irrigation/horticultural-crops/greenhouses.

Optik, P. G. . (2023). Optical transmission* of Schott WG225, WG280, WG295, WG305 and WG320. SCHOTT WG225, WG280, WG295, WG305, WG320, transmission [web page]. Retrieved from: https://www.pgo-online.com/intl/curves/optical_glassfilters/WG225_WG280_WG295_305_320.html.

Ouf, N. S. (2023). Leguminous seeds detection based on convolutional neural networks: Comparison of faster R-CNN and YOLOv4 on a small custom dataset. *Artificial Intelligence in Agriculture 8*, 30-45.

Pallottino, F., Antonucci, F., Costa, C., Bisaglia, C., Figorilli, S. & Menesatti, P. (2019). Optoelectronic proximal sensing vehicle-mounted technologies in precision agriculture: A review. *Computers and Electronics in Agriculture*, 162, 859-873.

Palum, R. *Conference Proceedings n°issue number*. *Image sampling with the Bayer color filter array*. PICS.

Pix4D-SA. (2023). Pix4D [web page]. Retrieved from: https://www.pix4d.com/industry/agriculture/.

plants LLC, S. (2022). Recommended Strawberry Varieties for Canada [web page]. Retrieved from: https://strawberryplants.org/recommended-strawberry-varieties-for-canada/#QC.

Purcell, C. R. (2000). *Remote sensing image performance metrics: Comparing ground sample distance and the national imagery interpretability rating scale*. California State University, Long Beach.

Ren, S., He, K., Girshick, R. & Sun, J. (2015). Faster r-cnn: Towards real-time object detection with region proposal networks. *Advances in neural information processing systems*, 28.

Sankaran, S., Khot, L. R., Espinoza, C. Z., Jarolmasjed, S., Sathuvalli, V. R., Vandemark, G. J., Miklas, P. N., Carter, A. H., Pumphrey, M. O. & Knowles, N. R. (2015). Low-altitude, high-resolution aerial imaging systems for row and field crop phenotyping: A review. *European Journal of Agronomy*, 70, 112-123.

Schaefer, H. M., McGraw, K. & Catoni, C. (2023). *web page n°issue number*. Birds use fruit colour as honest signal of dietary antioxidant rewards. Retrieved from: https://schott.com/shop/advanced-optics/en/Matt-Filter-Plates/N-WG2N-WG28080/c/glass-N-WG280.

Schaefer, H. M., McGraw, K. & Catoni, C. (2008). Birds use fruit colour as honest signal of dietary antioxidant rewards. *Functional Ecology*, 22(2), 303-310.

Senthilnath, J., Dokania, A., Kandukuri, M., Ramesh, K., Anand, G. & Omkar, S. (2016). Detection of tomatoes using spectral-spatial methods in remotely sensed RGB images captured by UAV. *Biosystems engineering*, 146, 16-32.

Shakhatreh, H., Sawalmeh, A. H., Al-Fuqaha, A., Dou, Z., Almaita, E., Khalil, I., Othman, N. S., Khreishah, A. & Guizani, M. (2019). Unmanned aerial vehicles (UAVs): A survey on civil applications and key research challenges. *Ieee Access*, 7, 48572-48634.

Song, J., Du, L., Li, L., Kalt, W., Palmer, L. C., Fillmore, S., Zhang, Y., Zhang, Z. & Li, X. (2015). Quantitative changes in proteins responsible for flavonoid and anthocyanin biosynthesis in strawberry fruit at different ripening stages: a targeted quantitative proteomic investigation employing multiple reaction monitoring. *Journal of proteomics*, 122, 1-10.

Stuart, M. B., McGonigle, A. J. & Willmott, J. R. (2019). Hyperspectral imaging in environmental monitoring: A review of recent developments and technological advances in compact field deployable systems. *Sensors*, 19(14), 3071.

Stumph, B., Virto, M. H., Medeiros, H., Tabb, A., Wolford, S., Rice, K. & Leskey, T. *Conference Proceedings n°issue number. Detecting invasive insects with unmanned aerial vehicles*. 2019 International Conference on Robotics and Automation (ICRA). IEEE.

Taguchi, H. & Enokido, M. (2017). Technology of color filter materials for image sensor. *Red*, 10502(8892), 3216.

Tsouros, D. C., Bibi, S. & Sarigiannidis, P. G. (2019). A review on UAV-based applications for precision agriculture. *Information*, 10(11), 349.

Ulizio, M. (2015). Optical Properties of Glass: How Light and Glass Interact [web page]. Retrieved from: https://www.koppglass.com/blog/optical-properties-glass-how-light-and-glass-interact.

Vanbrabant, Y., Delalieux, S., Tits, L., Pauly, K., Vandermaesen, J. & Somers, B. (2020). Pear flower cluster quantification using RGB drone imagery. *Agronomy*, 10(3), 407.

Wang, C., Wang, Y., Liu, S., Lin, G., He, P., Zhang, Z. & Zhou, Y. (2022). Study on pear flowers detection performance of YOLO-PEFL model trained with synthetic target images. *Frontiers in Plant Science*, 13.

Williams, H., Nejati, M., Hussein, S., Penhall, N., Lim, J. Y., Jones, M. H., Bell, J., Ahn, H. S., Bradley, S. & Schaare, P. (2020a). Autonomous pollination of individual kiwifruit flowers: Toward a robotic kiwifruit pollinator. *Journal of Field Robotics*, 37(2), 246-262.

Williams, H., Ting, C., Nejati, M., Jones, M. H., Penhall, N., Lim, J., Seabright, M., Bell, J., Ahn, H. S. & Scarfe, A. (2020b). Improvements to and large-scale evaluation of a robotic kiwifruit harvester. *Journal of Field Robotics*, 37(2), 187-201.

Zeng, Z., Wang, W. & Zhang, W. *Conference Proceedings n°issue number. Target classification algorithms based on multispectral imaging: A review*. 2021 6th International Conference on Multimedia and Image Processing.

Zheng, C., Abd-Elrahman, A. & Whitaker, V. (2021). Remote sensing and machine learning in crop phenotyping and management, with an emphasis on applications in strawberry farming. *Remote Sensing*, 13(3), 531.

Zhou, C., Lee, W. S. & Lin, R. *Conference Proceedings n°issue number. Strawberry Flower Detection using Fluorescence Imaging*. 2020 ASABE Annual International Virtual Meeting. American Society of Agricultural and Biological Engineers.

Zhou, Z., Majeed, Y., Naranjo, G. D. & Gambacorta, E. M. (2021). Assessment for crop water stress with infrared thermal imagery in precision agriculture: A review and future prospects for deep learning applications. *Computers and Electronics in Agriculture*, 182, 106019.

CONCLUSION AND RECOMMENDATIONS

This project challenged conventional ideas about remote sensing in agriculture by employing the visual range of insect pollinators in remote sensing of strawberry flowers. The objectives of this project were presented in two submitted publications. The article in Chapter 3 presents a meta-analysis of UV reflectance in remote sensing from 1969 to 2021. It revealed that UV reflectance is underutilized in crop studies as a remote sensing parameter. Most studies were lab-based and used spectrophotometers or spectrometers/spectroradiometers, which are impractical for precision agriculture. The studies with a "field" component used various camera models and setups. Although the cameras presented were costly and bulky, I identified a need for a lightweight, cost-effective camera which could capture near UV data. Furthermore, one of the highest global-producing crops, Strawberry, had yet to be spectrally analyzed. Using a spectrophotometer, I analyzed two species of Strawberry (*Fragaria vesca* and four *Fragaria x ananassa* cultivars). I made all spectrographs available in the Floral Reflectance Database (FReD). By calculating the contrast between floral parts and background leaves, I identified that the cultivar most noted for its high yield and fruit quality demonstrates the highest visibility to pollinators (bees). Higher pollination rates are known to affect strawberry fruit quality and size positively. Breeders of strawberry cultivars could have been selected for this parameter without knowing, as it is inconspicuous in the human visual spectrum. The second submitted publication in Chapter 4 presented the Nature-inspired detector (NID). The NID is a lightweight, inexpensive system which captures monochrome images in the visual spectrum of a bee (300-650nm) and detects strawberry flowers. Unlike visible spectrum RGB cameras, I designed the NID camera to allow wavelengths down to 300nm (near- UV) to reach the sensor. UV cameras are usually expensive and heavy. However, the NID was light enough to field test on a UAV over a strawberry field. The NID remote sensor (camera) shows a linear response for the near-UV to the visible spectrum, which was determined through characterization with custom UV standards and a spectrophotometer. The linear response denotes a direct relationship between a pixel value

captured by the NID and the imaged objects' percent reflectance. The second part of the NID is the algorithm which detects strawberry flowers. YoloV5 and Faster R-CNN are industry-standard detection algorithms for flower detection. To train these algorithms, I created an image dataset with the NID camera of white-flowering strawberry cultivars, which is publically available for future work (DOI:10.5281/zenodo.7863719). Once trained, the NID system was mounted on a UAV and deployed over a strawberry field in Quebec, Canada. YoloV5 outperformed Faster R-CNN in field trials in mean average precision (mAP) and image processing speed (FPS). When results from a similar publication (methodology and target species) using an RGB camera were compared to those from this study, the NID outperformed in training time, mAP and processing time (FPS). In conclusion, our NID system should be deployed in other agricultural settings, including greenhouses and polytunnels. It has potential use in crop breeding and pollinator interaction studies also. The NID flower image dataset and flower detection trained algorithms have room for improvement in future work. Adding more flower images and unripe fruit would increase the system's robustness and reduce false positive detections. Contributions to the Floral Reflectance Database (FReD) should be consulted for future works designing a remote sensor for strawberry flowers as it can inform the choice of spectral range needed. Overall, crop species should be included in spectral studies, especially in the near UV range. The effects of crop breeding should be assessed regarding visibility to natural pollinators, as agricultural fields comprise a large part of pollinator landscapes globally.

Bibliography

Amador, G. J. & Hu, D. L. (2017). Sticky solution provides grip for the first robotic pollinator. *Chem*, 2(2), 162-164.

Bandara, A. (2011). *A music keyboard with gesture-controlled effects based on computer vision*. (Thesis).

Bors, R. & Sullivan, J. (2005). Interspecific hybridization of Fragaria vesca subspecies with F. nilgerrensis, F. nubicola, F. pentaphylla, and F. viridis. *Journal of the American Society for Horticultural Science*, 130(3), 418-423.

Botta, A., Cavallone, P., Baglieri, L., Colucci, G., Tagliavini, L. & Quaglia, G. (2022). A review of robots, perception, and tasks in precision agriculture. *Applied Mechanics*, 3(3), 830-854.

Briscoe, A. D. & Chittka, L. (2001). The evolution of color vision in insects. *Annual review of entomology*, 46(1), 471-510.

Ceres, R., Pons, J., Jimenez, A., Martin, J. & Calderón, L. (1998). Agribot: A robot for aided fruit harvesting. *Industrial Robot*, 25(5), 337-346.

Cheein, F. A. A. & Carelli, R. (2013). Agricultural robotics: Unmanned robotic service units in agricultural tasks. *IEEE industrial electronics magazine*, 7(3), 48-58.

Chen, B., Jin, Y. & Brown, P. (2019). An enhanced bloom index for quantifying floral phenology using multi-scale remote sensing observations. *ISPRS Journal of Photogrammetry and Remote Sensing*, 156, 108-120.

Dyer, A. G., Muir, L. & Muntz, W. (2004). A calibrated gray scale for forensic ultraviolet photography. *Journal of forensic sciences*, 49(5), 1056-1058.

Erik. (2022). Recommended strawberry varieties for Canada. Strawberry Plants [Web Page]. Retrieved from: https://strawberryplants.org/recommended-strawberry-varieties-for-canada/#QC.

Garcia, J. E., Greentree, A. D., Shrestha, M., Dorin, A. & Dyer, A. G. (2014). Flower colours through the lens: quantitative measurement with visible and ultraviolet digital photography. *PloS one*, 9(5), e96646.

Gonzalez-de Soto, M., Emmi, L., Garcia, I. & Gonzalez-de Santos, P. (2015). Reducing fuel consumption in weed and pest control using robotic tractors. *Computers and electronics in agriculture*, 114, 96-113.

Gonzalez-de Soto, M., Emmi, L., Benavides, C., Garcia, I. & Gonzalez-de Santos, P. (2016). Reducing air pollution with hybrid-powered robotic tractors for precision agriculture. *Biosystems Engineering*, 143, 79-94.

GouvernementduCanada. (2022). Statistical Overview of the Canadian Fruit Industry 2020 [Web Page]. Retrieved from: https://agriculture.canada.ca/en/sector/horticulture/reports/statistical-overview-canadian-fruit-industry-2021#a1.4.

Guerra-Sanz, J. M. (2008). Crop pollination in greenhouses. *Bee pollination in agricultural ecosystems*, 27-47.

Hansen, C., Steinmetz, H. & Block, J. (2022). How to conduct a meta-analysis in eight steps: a practical guide [Journal Article]. Retrieved from: Springer.

Hummer, K. E., Bassil, N. & Njuguna, W. (2011). Fragaria//Wild Crop Relatives: Genomic and Breeding Resources. *Springer*.

Jianlun, W., Yu, H., Shuangshuang, Z., Hongxu, Z., Can, H., Xiaoying, C., Yun, X., Jianshu, C. & Shuting, W. (2016). A new multi-scale analytic algorithm for edge extraction of strawberry leaf images in natural light. *International Journal of Agricultural and Biological Engineering*, 9(1), 99-108.

Kattenborn, T., Leitloff, J., Schiefer, F. & Hinz, S. (2021). Review on Convolutional Neural Networks (CNN) in vegetation remote sensing. *ISPRS journal of photogrammetry and remote sensing*, 173, 24-49.

Kevan, P. G. & Viana, B. F. (2003). The global decline of pollination services. *Biodiversity*, 4(4), 3-8.

Koski, M. H. & Ashman, T.-L. (2015). An altitudinal cline in UV floral pattern corresponds with a behavioral change of a generalist pollinator assemblage. *Ecology*, 96(12), 3343-3353.

LDP.LLC-MAXMAX. (2019). Maxmax monochrome camera module [web page]. Retrieved from: https://maxmax.com/shopper/product/15991-xniteusb8m-m-usb-2-0-8megapixel-monchrome-camera-mod.

Lee, C., Kim, H. J. & Oh, K. W. *Conference Proceedings n°issue number. Comparison of faster R-CNN models for object detection*. 2016 16th international conference on control, automation and systems (iccas). IEEE.

Lin, P. & Chen, Y. *Conference Proceedings n°issue number. Detection of strawberry flowers in outdoor field by deep neural network*. 2018 IEEE 3rd International Conference on Image, Vision and Computing (ICIVC). IEEE.

Ma, K. Y., Chirarattananon, P., Fuller, S. B. & Wood, R. J. (2013). Controlled flight of a biologically inspired, insect-scale robot. *Science*, 340(6132), 603-607.

Mabberley, D. (2002). Potentilla and Fragaria (Rosaceae) reunited. *Telopea*, 9(4), 793-801.

Maes, W. H. & Steppe, K. (2019). Perspectives for remote sensing with unmanned aerial vehicles in precision agriculture. *Trends in plant science*, 24(2), 152-164.

Marta, A. E., Camadro, E. L., Díaz-Ricci, J. C. & Castagnaro, A. P. (2004). Breeding barriers between the cultivated strawberry, Fragaria× ananassa, and related wild germplasm. *Euphytica*, 136, 139-150.

Nguyen, T. T., Kayacan, E., De Baedemaeker, J. & Saeys, W. (2013). Task and motion planning for apple harvesting robot. *IFAC Proceedings Volumes*, 46(18), 247-252.

Nimmo, R. (2022). Replacing cheap nature? Sustainability, capitalist future-making and political ecologies of robotic pollination. *Environment and Planning E: Nature and Space*, 5(1), 426-446.

Ohi, N., Lassak, K., Watson, R., Strader, J., Du, Y., Yang, C., Hedrick, G., Nguyen, J., Harper, S. & Reynolds, D. *Conference Proceedings n°issue number*. *Design of an autonomous precision pollination robot*. 2018 IEEE/RSJ international conference on intelligent robots and systems (IROS). IEEE.

OMAFRA. (2022). Growing Strawberries for Home Gardeners [Web Page]. Retrieved from: https://www.ontario.ca/page/growing-strawberries-home-gardens.

Optik, P. G. . (2023). Optical transmission* of Schott WG225, WG280, WG295, WG305 and WG320. SCHOTT WG225, WG280, WG295, WG305, WG320, transmission [web page]. Retrieved from: https://www.pgo-online.com/intl/curves/optical_glassfilters/WG225_WG280_WG295_305_320.html.

Qu, Z., Gao, L.-y., Wang, S.-y., Yin, H.-n. & Yi, T.-m. (2022). An improved YOLOv5 method for large objects detection with multi-scale feature cross-layer fusion network. *Image and Vision Computing*, 125, 104518.

Rieseberg, L. H. & Schilling, E. E. (1985). Floral flavonoids and ultraviolet patterns in Viguiera (Compositae). *American journal of botany*, 72(7), 999-1004.

Rørslett, B. (2006). Flowers in ultraviolet arranged by Plant Family. Flowers in Ultra-Violet [Web Page]. Retrieved from: http://www.naturfotograf.com/UV_flowers_list.html.

Sanchez, S., Romero, H. & Morales, A. (2020). *A review: Comparison of performance metrics of pretrained models for object detection using the TensorFlow framework*. Conference Proceedings presented in IOP Conference Series: Materials Science and Engineering (pp. 012024).

Shaneyfelt, T., Jamshidi, M. M. & Agaian, S. (2013). A vision feedback robotic docking crane system with application to vanilla pollination. *International Journal of Automation and Control*, 7(1-2), 62-82.

Sishodia, R. P., Ray, R. L. & Singh, S. K. (2020). Applications of remote sensing in precision agriculture: A review. *Remote Sensing*, 12(19), 3136.

Sridevi, M. & Mala, C. (2012). A survey on monochrome image segmentation methods. *Procedia Technology*, 6, 548-555.

Tsouros, D. C., Bibi, S. & Sarigiannidis, P. G. (2019). A review on UAV-based applications for precision agriculture. *Information*, 10(11), 349.

Williams, H., Nejati, M., Hussein, S., Penhall, N., Lim, J. Y., Jones, M. H., Bell, J., Ahn, H. S., Bradley, S. & Schaare, P. (2020). Autonomous pollination of individual kiwifruit flowers: Toward a robotic kiwifruit pollinator. *Journal of Field Robotics*, 37(2), 246-262.

Wójtowicz, M., Wójtowicz, A. & Piekarczyk, J. (2016). Application of remote sensing methods in agriculture. *Communications in biometry and crop science*, 11(1), 31-50.

Yoshioka, Y., Horisaki, A., Kobayashi, K., Syafaruddin, Niikura, S., Ninomiya, S. & Ohsawa, R. (2005). Intraspecific variation in the ultraviolet colour proportion of flowers in Brassica rapa L. *Plant breeding*, 124(6), 551-556.

Yuan, T., Zhang, S., Sheng, X., Wang, D., Gong, Y. & Li, W. *Conference Proceedings n°issue number. An autonomous pollination robot for hormone treatment of tomato flower in greenhouse*. 2016 3rd international conference on systems and informatics (ICSAI). IEEE.

Zan, X., Zhang, X., Xing, Z., Liu, W., Zhang, X., Su, W., Liu, Z., Zhao, Y. & Li, S. (2020). Automatic detection of maize tassels from UAV images by combining random forest classifier and VGG16. *Remote Sensing*, 12(18), 3049.

Zhang, N., Wang, M. & Wang, N. (2002). Precision agriculture—a worldwide overview. *Computers and electronics in agriculture*, 36(2-3), 113-132.

Zhou, C., Lee, W. S. & Lin, R. *Conference Proceedings n° issue number. Strawberry Flower Detection using Fluorescence Imaging*. 2020 ASABE Annual International Virtual Meeting. American Society of Agricultural and Biological Engineers.